PROMOTioN
PROGRESS ON MESHED HVDC OFFSHORE TRANSMISSION NETWORKS

D10.4: Document on Test Result Analysis

PROMOTioN – Progress on Meshed HVDC Offshore Transmission Networks
Mail info@promotion-offshore.net
Web www.promotion-offshore.net

This result is part of a project that has received funding form the European Union's Horizon 2020 research and innovation programme under grant agreement No 691714.

CONTACT

DOCUMENT INFO SHEET

Document Name:	Document on Test Result Analysis
Responsible partner:	DNV GL
Work Package:	WP10
Work Package leader:	Rene Smeets
Task:	10.4
Task lead:	Nadew Belda

DISTRIBUTION LIST

PROMOTioN Partners, European Commission

APPROVALS

	Name	Company
Validated by:	Fisnik Loku, Philipp Ruffing	RWTH Aachen
Task leader:	Nadew Belda	DNV GL
WP Leader:	Rene Smeets	DNV GL

DOCUMENT HISTORY

Version	Date	Main modification	Author
1.0	04-03-2019	First draft	Nadew Belda
2.0	14-03-3019	Final draft	Nadew Belda
3.0	09-04-2019	Minor comments	Nadew Belda

WP Number	WP Title	Person months	Start month	End month
10	Circuit Breaker Performance Demonstration	60	25	48

Deliverable Number	Deliverable Title	Type	Dissemination level	Due Date
10.4	Document on Test Result Analysis	Report	Public	39

LIST OF CONTRIBUTORS

Work Package and deliverable involve a large number of partners and contributors. The names of the partners, who contributed to the present deliverable, are presented in the following table.

PARTNER	NAME
DNV GL, KEMA Laboratories	Nadew Belda, Cornelis Plet, Rene Smeets, Roy Nijman,

CONTENT

This project has received funding from the European Union's Horizon 2020 research and innovation programme under grant agreement No 691714.

This project has received funding from the European Union's Horizon 2020 research and innovation programme under grant agreement No 691714.

ABBREVIATIONS

HVDC – High-voltage direct current

DC CB – direct current circuit breaker

TIV – Transient Interruption Voltage

MOSA – Metal Oxide Surge Arresters

PT – Power Transformers

TSG – Triggered spark gap

DS – Disconnecting switch

ES – Earthing Switch

CZC – Current Zero Crossing

VCB – Vacuum Circuit Breakers

VI – Vacuum interrupter

This project has received funding from the European Union's Horizon 2020 research and innovation programme under grant agreement No 691714.

EXECUTIVE SUMMARY

This document provides detailed analysis of current interruption test results of an experimental DC CB with active current injection set-up in a test laboratory. First, the test arrangement of the experimental DC CB is discussed. Then, the test method and test procedure are briefly presented.

Three test duties, namely, test duty 1, 2 and 3 with interruption current magnitudes of 2, 10 and 16 kA, respectively, are defined. Different configurations of a test circuit are designed to supply these test duty currents at different energy levels. The current interruption performances of three different, commercially available, types of vacuum circuit breakers (VCBs) are investigated for the defined test duties. In fact, the investigation is only on the vacuum interrupters of these CBs. First, the parameters that have a strong impact on the current interruption performance of vacuum interrupters (VIs) are identified. These parameters include the duration of arcing until current zero crossing (CZC), the rate-of-change of current at CZCs, and the initial and the peak values of the transient interruption voltage (TIV). In addition, the possible events after CZCs such as reignition and restrike are discussed in detail together with their possible causes.

For the three different types of VCBs, two set-ups; the first using a single interrupter and the other is using double interrupters are arranged. All test duties are performed at least 10 times for each set-up and for each VCB type. As much as possible, the current injection circuit parameters remain the same for all the VCB types in order to make a fair comparison. Critical test results have been plotted and the detailed phenomena during the current interruption process are explained for each case.

Analysis of the test results shows that the three different types of VIs used in the investigation perform in a completely different manner when interrupting DC currents. This indicates a strong impact of the VI contact design, contact material and composition. For example, VCB type A, which is a 38 kV, 31.5 kA AC VCB, rarely interrupts current on the first CZC regardless of the length of arcing duration. This VCB mainly interrupts the current on the even numbered CZCs which occur after minor loop (half cycle) current flow. On the other hand, the VCB type B, which is a 36 kV, 40 kA AC VCB, mainly clears on the 1st CZC. Reignitions occurred only on a few occasions and were subsequently cleared on later CZCs. Moreover, the third type of VCB, which is 36 kV, 31.5 kA AC VCB, only clears on the 1st CZC. It never cleared when reignition occurred on the 1st CZC or when a restrike occurred afterwards. To illustrate these and other conclusions, a statistical analysis of the test results is presented. The main conclusion from this investigation is the fact that the vacuum interrupters can be optimized for DC current interruption.

The stresses on the metal oxide surge arrester (MOSA) during current interruption are also analysed in detail. Robust design of MOSA for DC CB application is essential. Custom-made surge arrester banks, allowing the measurement of temperature and current through the individual surge arrestor columns, were used for the realisation of the experimental DC CB. Current sharing among the MOSA columns and the temperature of the MOSA after successive current interruptions are discussed. It is found out that the MOSA could sustain energy injection even after heated to more than 200 ºC. There was not a major current sharing issue observed during the test campaign.

This project has received funding from the European Union's Horizon 2020 research and innovation programme under grant agreement No 691714.

1 INTRODUCTION

1.1 PURPOSE

The purpose of this document is to present the detailed analysis of the current interruption process of an experimental mechanical DC CB, with active current injection scheme set up in a laboratory environment. Test results including test failure cases are discussed without any restriction. To get an insight of the stresses on internal sub-components, internal measurements of the experimental DC CB including current and voltage measurements through various parts are discussed. In-depth analysis of stresses on the VI(s) such as voltage, current and rate-of-change of current near current zero are presented. In addition, a special focus is given to the MOSA for DC CB applications. The overall energy absorption capability and energy sharing among multiple columns of MOSA are presented.

Later, within WP10, the results of this investigation serve as inputs for failure mode analysis which focuses on the HVDC CBs subcomponents failures and subsequent impacts. Moreover, the test results are made available to work package 6 of the PROMOTioN project to validate their software models of DC CB and its internal components.

1.2 MOTIVATION

In order to evaluate the interaction of the DC CBs with their electrical environment, it is necessary to get access to the internal measurements in addition to the current through and voltage across the overall DC CB. Because of the confidentiality issues, it is inconvenient to publicly discuss the internal measurements of the manufacturer's DC CBs tested within the project consortium. Thus, the motive for setting up the experimental DC CB is to be able to investigate the performance limits of the internal components and publish the test results without jeopardizing the manufacturers confidential information. Moreover, the tests are performed under real power condition where the components are subjected to proper stresses as would be expected in a practical operation. This provides exceptional platform for quantifying the stresses on the individual internal components of the DC CB; hence, providing hands on experience with testing this equipment. Meanwhile, the experience gained serves as input for test requirement specification for the DC CB to be demonstrated within the project. The test results provide guidelines for the test procedure.

1.3 DOCUMENT STRUCTURE

In chapter 2 the experimental DC CB test set-up is discussed together with a brief review of test methods and test procedures. The detailed analysis of a number of unique test results are discussed in Chapter 3, in which test results obtained using single break as well as double break DC CBs, using various vacuum interrupters, are discussed. Moreover, microscopic phenomena in a vacuum interrupter near current zero are elaborated through a closer look at the measurements. The stresses on the metal oxide surge arrester (MOSA), current through some columns and temperature rise of some columns over a quick succession of tests are presented. In chapter 4, summary of the deliverable is provided.

This project has received funding from the European Union's Horizon 2020 research and innovation programme under grant agreement No 691714.

2 EXPERIMENTAL DC CB

2.1 TEST SET-UP

The test is set up using standard components available in the test laboratory as shown in Figure 2-1. On the left side of this figure is a power source consisting of AC short-circuit generators operated at reduced power frequency. One or more short-circuit generators are used to supply the necessary power, current and energy stresses during the test. Several short-circuit transformers are used to step-up the source voltage to the desired level in relation to the DC CB TIV rating. Next to the power transformers (PTs) is a triggered spark gap (TSG1) in parallel connection not only with the power source but also with the experimental DC CB (see red dashed box) as shown in the middle of Figure 2-1. This is intended to protect the power source and the components of the experimental DC CB against any unforeseen overvoltage conditions. Normally in a complete test circuit (planned for the test objects from manufacturers), the TSG1 is used in combination with an auxiliary AC circuit breaker (connected in series with the test object) for over-current protection. This is discussed in detail in deliverable 10.1, [1].

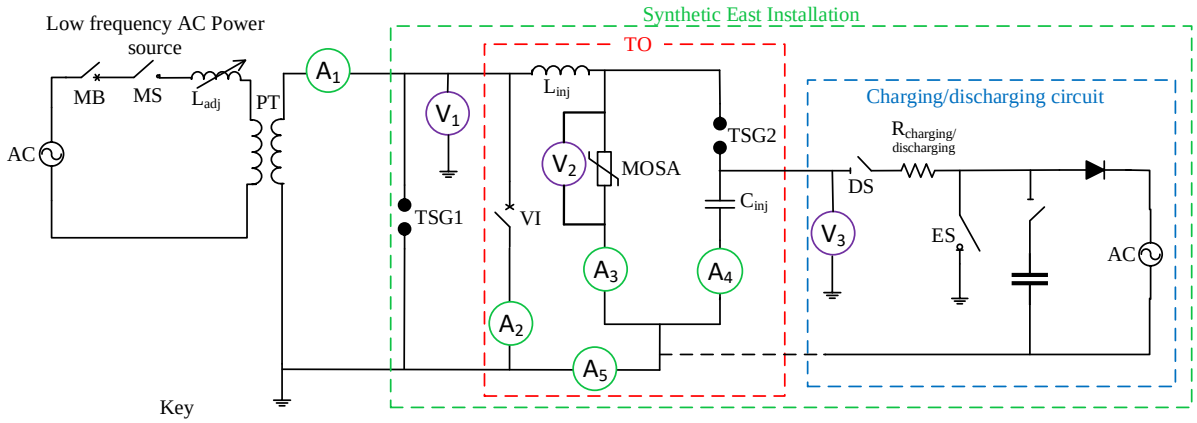

Key

MB= Master Breaker
MS= Making Switch
L_{adj}= adjustable reactor
PT= Power Transformer(s)
VI=Vacuum Interrupter
A = current measurement
V = voltage measurement

MOSA= Metal oxide surge arrester
C_{inj}=counter current injection capacitor
L_{inj}=counter current injection inductor
DS=Disconnector switch
ES=Earthing switch
TSG=Triggered Spark Gap (Triggered make gap)
$R_{charging/discharging}$ = charging and discharging resistor

Figure 2-1: Single line diagram of test set-up

The main components of the experimental DC CB are shown in the dashed red box in the centre of Figure 2-1. It consists of a vacuum circuit breaker (VCB) as the current interrupter in the main current path, a pre-charged capacitor (C_{inj}) which supplies a counter injection current, an injection circuit inductor (L_{inj}) which is used to limit the peak value and frequency of the counter injection current, the triggered spark gap 2 (TSG2) that serves as a high-speed making switch and finally the MOSA (metal oxide surge arrester), which is a crucial component for limiting and maintaining the voltage across the DC CB; and absorbing the energy in the circuit during current suppression.

This project has received funding from the European Union's Horizon 2020 research and innovation programme under grant agreement No 691714.

In the arrangement depicted in Figure 2-1 the MOSA is in parallel with the injection capacitor. It could be connected in parallel with the VCB; however, in that case, during current commutation into the MOSA there will be some damped high-frequency voltage overshoot due to the fact that by the time the capacitor is charged to the clamping voltage level, the system current still flows through the injection reactor. Since the commutation of current from a reactor is not instant, the capacitor keeps charging until the current commutation from the reactor is over. This voltage also appears across the VI of the VCB. Therefore, to slightly reduce the voltage stress on the VI, the arrangement shown in Figure 2-1 is chosen. In this case there is no need to commutate current from the injection reactor during the entire current suppression period (when the MOSA is conducting). This will be discussed in detail in Chapter 3.

The circuit on the right most side of Figure 2-1 is the charging and discharging circuit for the injection capacitor of the experimental DC CB which is performed just before and after a test sequence is started and finished, respectively.

In addition, there are current measurements in each path and the voltage measurements across the VI, across the MOSA as well as across the entire test object as seen by the test circuit are shown in Figure 2-1. The MOSA branch has multiple columns each providing a current path during energy absorption/current suppression. There are current measurements through some of the columns (up to 8-channels) which are not shown on the single line diagram of Figure 2-1. Furthermore, there are 8 optical based temperature sensors attached to 8 columns of the MOSA which are not shown in the diagram.

2.2 SINGLE INTERRUPTER AND DOUBLE INTERRUPTER EXPERIMENTAL DC CB SET-UPS

The performance of a VI in different stages of the current interruption process depends on the contact design, contact materials, contact composition, etc. In order to consider the impacts of the differences in the design of VI contacts, three standard off-the-shelf VCBs produced by various manufacturers are used. The VCBs used in the experimental DC CB are all three-phase AC circuit breakers with ratings shown in Table 1.

Table 1: Specifications of VCBs used in the experimental DC CB

VCB type	Voltage rating (kV_{RMS})	Current rating (kA_{RMS})	Short-circuit current rating (KA_{RMS})	Opening time (ms)	Operation mechanism	Previous use
Type A	38	2.5	31.5	37	Independently controlled poles	new
Type B	36	2.5	40	46.6	Common drive (spring)	used
Type C	36	2.0	31.5	37	Common drive (spring)	used

Moreover, when designing the experimental DC CB, the TIV rating is decided based on the AC rating of the used vacuum circuit breakers. The AC voltage rating of the used VCBs fall in the range between 36-38 kV (RMS, for

This project has received funding from the European Union's Horizon 2020 research and innovation programme under grant agreement No 691714.

AC application) as shown in Table 1. In order not to exceed the AC voltage ratings, the equivalent voltage for a single interrupter experimental DC CB is chosen to be 40 kV with transient overshoots as high as 45 kV.

For the single interrupter case, only one out of the three poles (VIs) is used while the remaining poles are not connected to the circuit. A single line diagram for a single interrupter experimental DC CB set-up is shown in Figure 2-2a. In order to double the voltage rating (thus, the TIV) of the experimental DC CB, two VIs are connected in series as shown in Figure 2-2b. To ensure the doubling of the TIV, two series connected MOSA stacks are used. The current rating remains the same as for the single interrupter case. Nevertheless, the charging voltage of the injection capacitor, the capacitance and the inductance in the injection branch are adjusted to keep the electrical stresses of the components the same as for the single interrupter case. The parameter values of the injection circuit components and the resulting rate-of-change of current through the VIs while interrupting different current duties is shown in Table 2 and Table 3 for single and double interrupter set-ups, respectively.

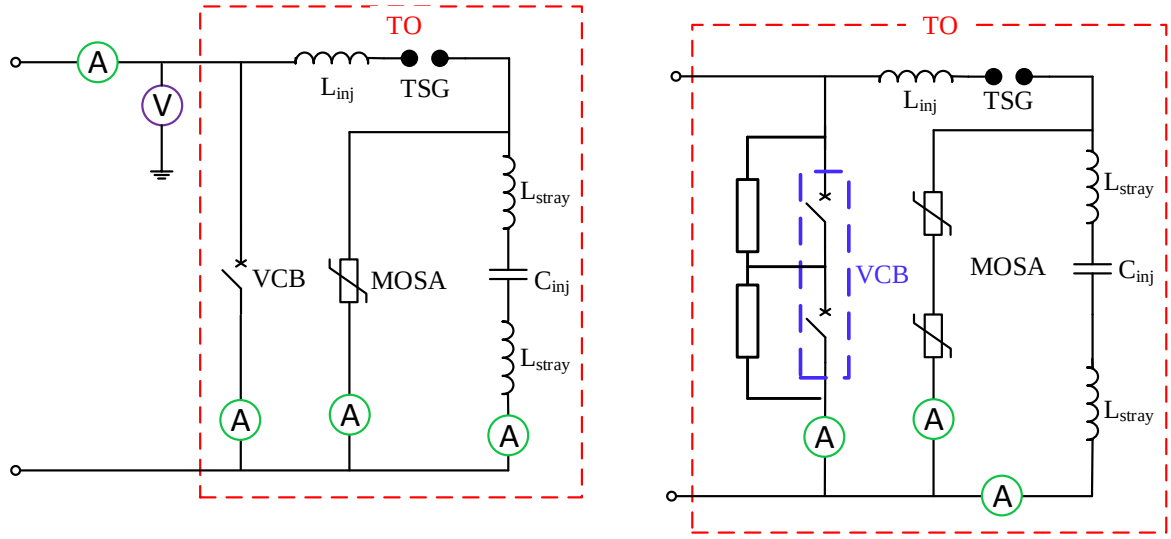

a) Single interrupter module

b) Double interrupter module

Figure 2-2: Single line diagrams of a single interrupter and double interrupter experimental DC CB

For the double (multi-) interrupter set-up there are additional components, namely, the voltage grading elements across each VI to ensure equal TIV distribution. Grading capacitors are used in the experimental campaign. The effectiveness of different values of grading capacitors is investigated and this is discussed in Chapter 3.

Table 2: Injection circuit parameters of single interrupter experimental DC CB

Frequency (kHz)	1.0	2.0	3.0	4.0	5.0	6.0	7.0	8.0	9.0	10.0
Capacitor (µF)	127.3	63.7	42.4	31.8	25.5	21.2	18.2	15.9	14.1	12.7
Inductor (µH)	199.0	100.0	66.3	49.7	39.8	33.2	28.4	24.5	22.1	20.0
di/dt @2 kA (kA/µs)	0.125	0.250	0.375	0.500	0.625	0.750	0.875	1.00	1.125	1.250
di/dt @10 kA (kA/µs)	0.109	0.218	0.327	0.435	0.544	0.653	0.762	0.871	0.980	1.088
di/dt @16 kA (kA/µs)	0.075	0.151	0.226	0.302	0.377	0.452	0.528	0.603	0.679	0.754

This project has received funding from the European Union's Horizon 2020 research and innovation programme under grant agreement No 691714.

Table 3: Injection circuit parameters for double interrupter experimental DC CB

Frequency (kHz)	1.0	2.0	3.0	4.0	5.0	6.0	7.0	8.0	9.0	10.0
Capacitor (µF)	63.66	31.83	21.22	15.92	12.73	10.61	9.09	7.96	7.07	6.37
Inductor (µH)	398	199	132.6	99.5	79.6	66.3	56.8	49.7	44.2	39.8
di/dt @2 kA (kA/µs)	0.130	0.260	0.389	0.519	0.649	0.778	0.908	1.038	1.167	1.297
di/dt @10 kA (A/µs)	0.113	0.226	0.339	0.452	0.565	0.678	0.791	0.904	1.017	1.130
di/dt @16 kA (A/µs)	0.081	0.162	0.243	0.325	0.406	0.488	0.569	0.650	0.731	0.812

2.3 TEST METHOD AND TEST PROCEDURE

The experimental DC CB is set up with a focus on the investigation of stresses on internal subcomponents. The overall performance, specifically the speed of operation of the DC CB is not the main objective here. This is due to the fact that the components of the experimental DC CB, specifically the mechanism/drives of the vacuum circuit breakers used are not designed for DC CB application, but for AC CB application which is slower.

The test parameters, however, are the same parameters used for testing a real DC CB. An example demonstrating the prospective current produced during a test is shown in Figure 2-3 together with number of timing signals. The test object (the experimental DC CB) is operated in such a way that the contacts of the vacuum interrupter are separated after the prospective current starts to flow. This means that the vacuum circuit breaker needs to be tripped prior to the onset of the prospective current flow, as shown diagram of Figure 2-3. During testing of a real DC CB, the trip command to the DC CBs of manufacturers' is sent after short-circuiting is applied to mimic the actual situation in a practical application. In other words, the trip command signal is in the positive time in reference to Figure 2-3. The breaker opening time which is duration from the trip command and the moment of contact separation is precisely known for a vacuum circuit breaker, see Table 1. Therefore, it can be precisely sequenced with the moment of short-circuit making as illustrated in Figure 2-3. The contact travel time which is from the contact separation until the contacts are fully open takes about 20-30 ms. However, this is not relevant here as the focus mainly during the contact travel period.

Given a test duty, test parameters of interest such as arcing duration until current zero creation, i.e. the time difference between the steps in the blue trace and the magenta trace in the diagram of Figure 2-3, can be controlled and varied precisely by adjusting the trip command in refence to the other timing signals. In Figure 2-3 T_{trip} is floating to show that this is one of the main parameters to adjust during the test campaign. Arcing duration until current zero creation is one of the crucial parameters determining the performance of the vacuum interrupter of a DC CB. It is related to the gap length between the contacts and hence, dielectric recovery of the vacuum interrupter when the current zero is created, although the latter does not have a linear relationship with the gap length. The detail of important parameters and their impact on the performance of DC CBs is discussed in Chapter 3.

In fact, in order to determine the impacts of these parameters, it is necessary to quantify and set these parameters in advance. Hence, before the actual test, there are necessary calibration steps aimed at precisely determining

This project has received funding from the European Union's Horizon 2020 research and innovation programme under grant agreement No 691714.

and setting the test parameters as well as the test duty current. These steps have been discussed in [1], [2] and [3] in detail and are briefly revised below for the sake of completeness of the document.

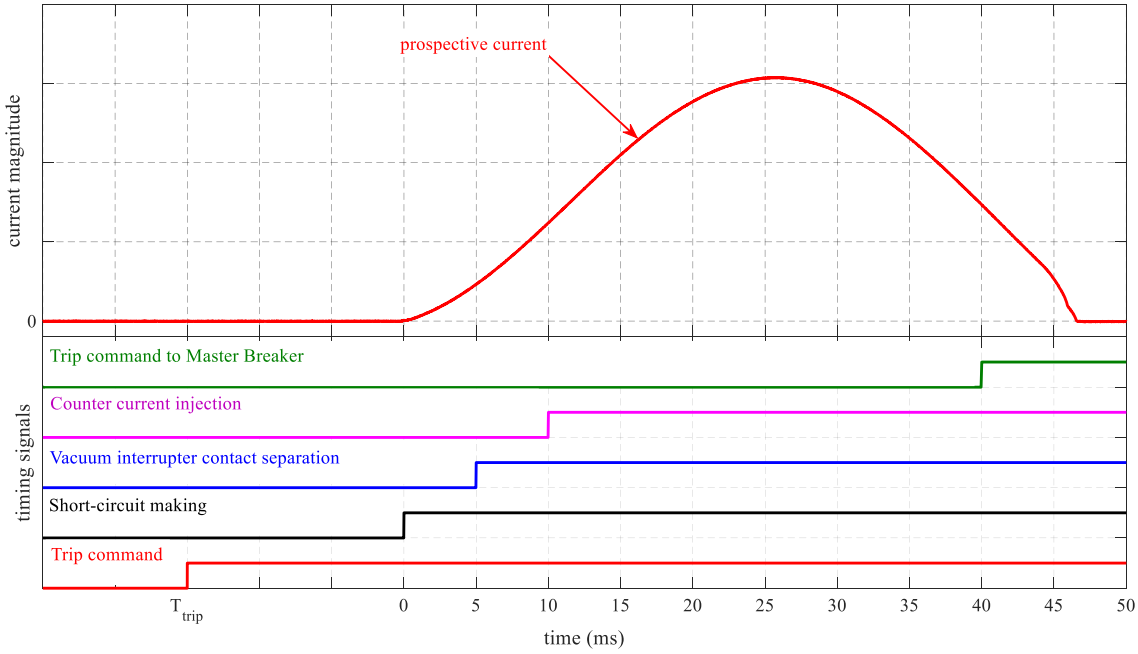

Figure 2-3: Graphical representation of test procedure and demonstration of timing sequence

Note that: The main differences between the normal DC CBs and the experimental DC CB discussed here are the opening time and the contact separation speed of the VIs. The opening time is disregarded as this can be taken into account by pre-tripping the VCB as shown in Figure 2-3. However, the contact moving speed cannot be accounted for here. This means the contact gap distance within certain arcing duration is not the same for the normal DC CBs which have special drive mechanism and the experimental DC CB which is based on AC VCBs. Certainly, this has an impact on the performance (not in quite well understood though) ; however, it is not only the contact gap distance but also certain minimum time until the vacuum arc gets conditioned, for example, until the arc diffuses across the contact surface that affects the interruption performance. Especially, the arc control becomes critical when the interruption current exceeds 10 kA [4]. This is reflected in the test results discussed in Chapter 3. For AC application minimum arcing duration is defined despite contact separation speed [4].

2.3.1 TEST OBJECT CALIBRATION

1. No load check - Checking of the Operation of VCB (open and close command)
   - Helps to determine the proper operation and measure the duration between trip command and the moment of contact separation
   - No generator energization is needed at this step
2. Injection circuit check - Capacitor charging/discharging check (VCB remain closed)
   - Helps to check the charging of the capacitor

This project has received funding from the European Union's Horizon 2020 research and innovation programme under grant agreement No 691714.

- Check counter injection current (peak and frequency). This helps to determine if any adjustment is needed in the injection circuit reactor since the magnitude of the parasitic/stray inductance is not yet known.
- Check discharging circuit for safety after current interruption is performed
- No generator energization is needed at this step

2.3.2 TEST CIRCUIT CALIBRATION

1. Prospective current check - Supply one loop[1] current to the test object from generators
   For example, for single break unit, the following test circuit parameters are required
   - Set frequency (e.g. 16.7 Hz, 30 Hz),
   - Set excitation voltage (e.g. 11.3 kV for single interrupter DC CB) and
   - Making angle (e.g. 20^0)
   - Check the di/dt
2. Set master breaker timer signal – This is to ensure the operation of master breakers to allow only one loop of current (see Figure 2-3)

2.3.3 COMBINED CALIBRATION OF TEST CIRCUIT AND TEST OBJECT

1. Combined generator current and counter-injection current check (VI remain closed, Master breaker operated)
2. Check number of zero-crossings: check the peak value of current if interrupted at first current zero (this corresponds to the test duty)
3. Adjust trip timer command to the test object (contact separation starts 2-4 ms after short-circuit making)
4. Adjust timer for triggered spark gap with reference to moment of contact separation

2.3.4 INTERRUPTION TESTS OF EXPERIMENTAL DC CB

This is the same as step 4 except the trip command is sent to VCB

- Check the arcing duration until current injection
- Measure the arcing duration until current interruption
- Check the residual voltage across the injection capacitor at interruption
- Check reignition voltage if it occurs
- Measure the di/dt at CZC

- Note: The arcing duration from the moment of contact separation up to triggering of spark gap for counter current injection is pre-set. However, due to some jitter it is always verified after test from measurements
- If counter current injection frequency is changed, only steps 2 and 4 are repeated

[1] current loop is one half cycle of a current. The current flow could be asymmetrical due to some DC offset resulting in minor loop and major loop current.

This project has received funding from the European Union's Horizon 2020 research and innovation programme under grant agreement No 691714.

- If the test duty is changed, steps 2-4 are repeated

2.4 TEST DUTIES AND TEST PARAMETERS

The stresses seen by one or more VI(s) when interrupting current depends on the current magnitudes. For example, it does not mean that a low current interruption is easier for the VI(s). For this reason, three test duties have been defined as shown below to investigate the impact of interruption current magnitude on the performance of VI(s).

- Test duty 1 – 2 kA current interruption
- Test duty 2 – 10 kA current interruption
- Test duty 3 – 16 kA current interruption

In fact, there are several parameters whose impacts are investigated at each current interruption test duty. For each test duty, tests are repeated 10 times by keeping circuit breaker parameters under investigation unchanged, for example, at a given arcing duration.

This project has received funding from the European Union's Horizon 2020 research and innovation programme under grant agreement No 691714.

3 TEST RESULTS ANALYSIS OF THE EXPERIMENTAL DC CB

The main components of a DC CB that are of interest to investigate are the vacuum interrupter (VI) and the metal oxide surge arrester (MOSA). The VI forms a key part of many types of HVDC CBs such as the active current injection DC CB and the VSC assisted resonant type DC CB, where in both cases it serves as the main local current interrupter [1], [5]- [6]. A brief description of the VIs used in the experimental investigation is presented in deliverable D10.2. The MOSA is another crucial component of any type of DC CBs including hybrid HVDC CBs, passive resonant DC CBs and pure power electronic DC CBs. During the DC current interruption, the MOSA serves as the component to limit and maintain the desired counter voltage (TIV) to suppress the fault/short-circuit current. In doing so, it absorbs several Mega Joules (MJs) of energy from the system in which the DC CB is located. The description and the design procedure of MOSA for HVDC CB application is discussed with sufficient detail in deliverable D10.2. In this chapter, the actual stresses on these components as observed from test results under various test conditions are presented.

3.1 ANALYSIS OF VACUUM INTERRUPTER STRESSES

For a VI to achieve DC current interruption, a current zero must be created through its opened contacts. Different technologies of DC CBs employ various techniques to achieve local current zeros through the VI. Nevertheless, at current zero, the VI must be able to deal with electrical, mechanical as well as thermal stresses to achieve successful local current interruption. Several variables of a system (in this case a test circuit) and the DC CB itself determine the possibility of interruption at current zero. These parameters are discussed in the following subsection.

3.1.1 MAIN PARAMETERS HAVING STRONG IMPACT ON CURRENT INTERRUPTION AT CURRENT ZERO

During the experimental tests, the impacts of several parameters are studied by precisely varying one or more parameter(s) at a time. Figure 3-1 shows current supplied by a test circuit and current flowing through the vacuum interrupter when a high-frequency current is super imposed from the discharge of a pre-charged capacitor. In order to show the CZCs, a zoomed in view of the current through the VI is shown. In this case the high-speed making switch represented by TSG2, see in Figure 2-1, is fired when the system current reaches 10 kA (test duty 2), thus injecting a high-frequency current. The frequency of the injection current is 4 kHz with a peak value of 20 kA (± 5%). In this case, the VI is intentionally kept in closed state. Due to inherent losses (i^2R) the current from the injection circuit decays quickly while the system current keeps rising. This limits the number of CZCs that can be created when interrupting rising current. In the example case shown in Figure 3-1, 13 CZCs are created, i.e. the VI had 13 chances to clear the local current had it been tripped to open its contacts during this period. Current zeros are shown by blue circles in the zoomed plot of Figure 3-1. The impacts of the following parameters are investigated during the experimental test campaign.

This project has received funding from the European Union's Horizon 2020 research and innovation programme under grant agreement No 691714.

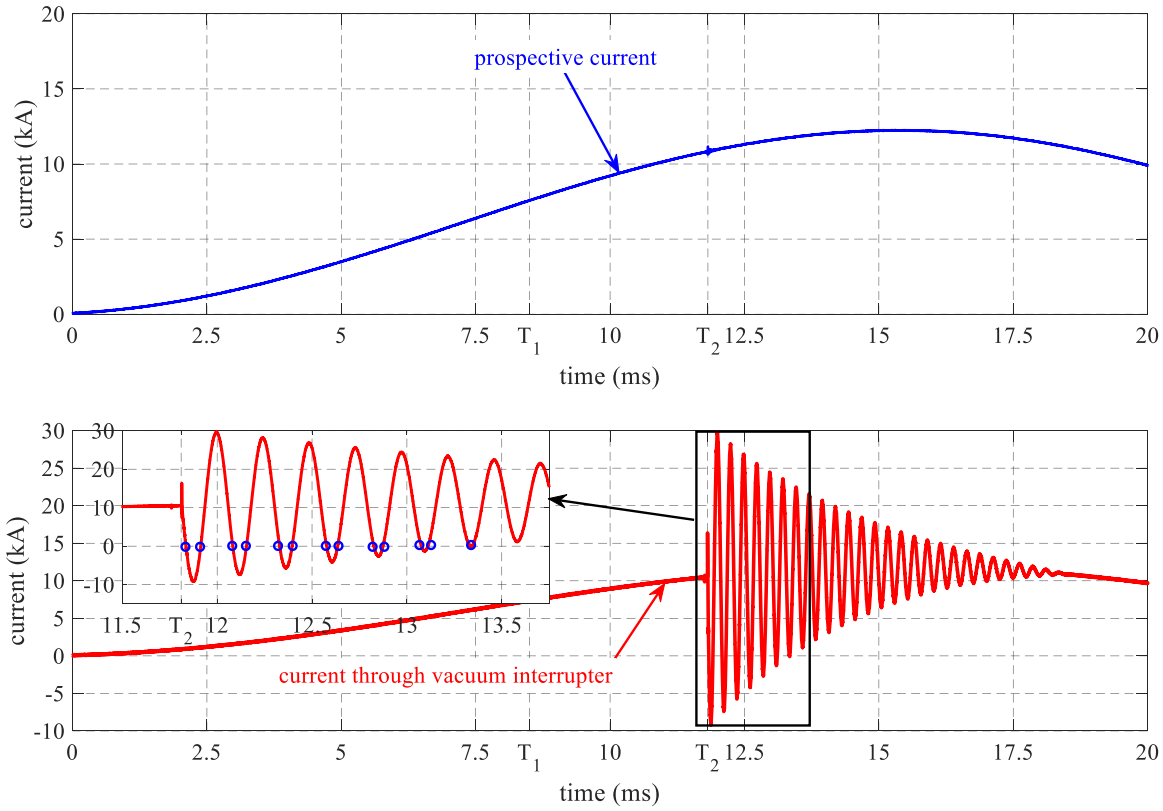

Figure 3-1: Typical prospective current and current through vacuum interrupter when current is injected while the VI remains closed

Arcing duration: - The duration between the moment of contact separation until the first current zero creation. In Figure 3-1, the time "T_1" designates the moment of contact separation and the time "T_2", is the moment of current injection. Thus, the arcing duration is from T_1 until a few tens of micro seconds after T_2. By adjusting the moment of contact separation (T_1) relative to T_2 (or vice versa) the arcing duration is varied to study its impacts in the VI performance. In most cases, as discussed later, the VI does not clear on the first current zero. Rather it could clear on later current zeros as the oscillation from the current injection branch continues. In the latter case the arcing duration from contact separation until each current zero including the final interruption or failure is determined from the measurements.

Rate-of-change of current near current zero (di/dt): - This is another crucial parameter determining the chance of successful local current interruption. The rate-of-change of current near CZC is determined by the frequency of the injection current, the peak value of the injection current and the magnitude of the system current to be interrupted. Given a peak value of the injection current, the higher the frequency of the injection current, the higher the di/dt at CZC when interrupting a given test current. In addition, at a given frequency and peak value of injection current, the lower the test duty current, the higher the di/dt at CZC. Without any aid from other circuit components (such as saturable reactor), the maximum rate-of-change of current at which the VI is capable of clearing is limited. It depends on several design parameters of the VI itself such as the contact design, material composition, etc. Normally, to achieve current interruption at CZC, saturable reactors are used to limit the rate-of-change of current near CZC while having limited impact (due to saturation) when the normal DC current is flowing through the VI.

This project has received funding from the European Union's Horizon 2020 research and innovation programme under grant agreement No 691714.

An important observation from Figure 3-1 is that the di/dt decreases over time. This is due to decay of the injection current magnitude caused by inherent ohmic losses and also due to slight increase in the system current. Thus, if the VI fails to clear on the first CZC, the chance that it clears on the subsequent CZCs increases from the di/dt stress point of view. This is also supplemented by the fact that the contact gap distance of the VI increases in the meantime. This is discussed in the next sections.

Maximum current interruption capability: - The peak value of system current that a VI can clear within a certain arcing duration is limited. First of all, given a design of a DC CB, the magnitude of the short-circuit current that can be interrupted cannot exceed the peak value of the injection current since CZCs cannot be created otherwise. In addition, even if a few CZCs can be created, the maximum current that the VI is capable of clearing is limited by thermal energy accumulated in the arc. Thus, given the arcing duration, the higher the current, the higher the thermal energy which enhances the chance of thermal reignition.

Vacuum interrupter design: - in order to investigate the differences in the interruption performance of different designs of a VI, three commercially available VCBs from different manufacturers are used in the test campaign. Although the internal design cannot be disclosed due to intellectual property issues, clear differences in the interruption performance is observed among the tested VIs.

Moreover, the impacts of some other electrical parameters such as the duration and the peak value of a loop current just before CZC when the VI fails to clear at the 1st CZC, the magnitude of the initial TIV (ITIV) due to remaining charge across the injection capacitor at CZC are investigated from the test results. As a result of the failure to withstand the above stresses, the VI can experience a reignition or restrike as discussed below.

Reignition: - occurs when the VI fails to clear at CZC or fails to sustain the ITIV that appears after interruption at CZC. This occurs when one/more of the above parameters reach the limit of the VI, for example, too short contact gap and/or arcing duration, too high di/dt or too large thermal energy in the arc as a result of too high current or combination of these. It could be thermal re-ignition due to high thermal energy in the arc plasma prior to CZC which persists during CZC or it could be dielectric re-ignition which results when vacuum gap is unable to sustain the TIV voltage just after CZC.

Restrike: - in some cases the vacuum interrupter breaks down dielectrically after current is commutated to the MOSA branch. In this case, it fails to sustain the continuous TIV voltage which is maintained by the MOSA until the energy in the circuit is absorbed. Re-strike could occur after current suppression is over when the DC CB is subjected to the system DC voltage. The latter is not investigated in the experimental test campaign.

In the proceeding sections, current interruption by DC CB modules with a single VI and double VIs in series are discussed. In order to observe the impact of using multiple VIs in series, the critical parameters are kept similar as for a single interrupter case. The current injection circuit parameters and the expected rate of change of current near CZC for both single interrupter and double interrupter cases are shown in Table 2 and Table 3.

3.1.2 TEST RESULTS ANALYSIS OF A SINGLE INTERRUPTER EXPERIMENTAL DC CB – VCB TYPE A

A single line diagram of a single interrupter experimental DC CB is described in Chapter 2 as shown in Figure 2-2a. The photo of the actual test set-up in the test laboratory is shown below in Figure 3-2 with the main components labelled on the photo. The injection capacitor is standing out of sight next to the experimental set-up.

This project has received funding from the European Union's Horizon 2020 research and innovation programme under grant agreement No 691714.

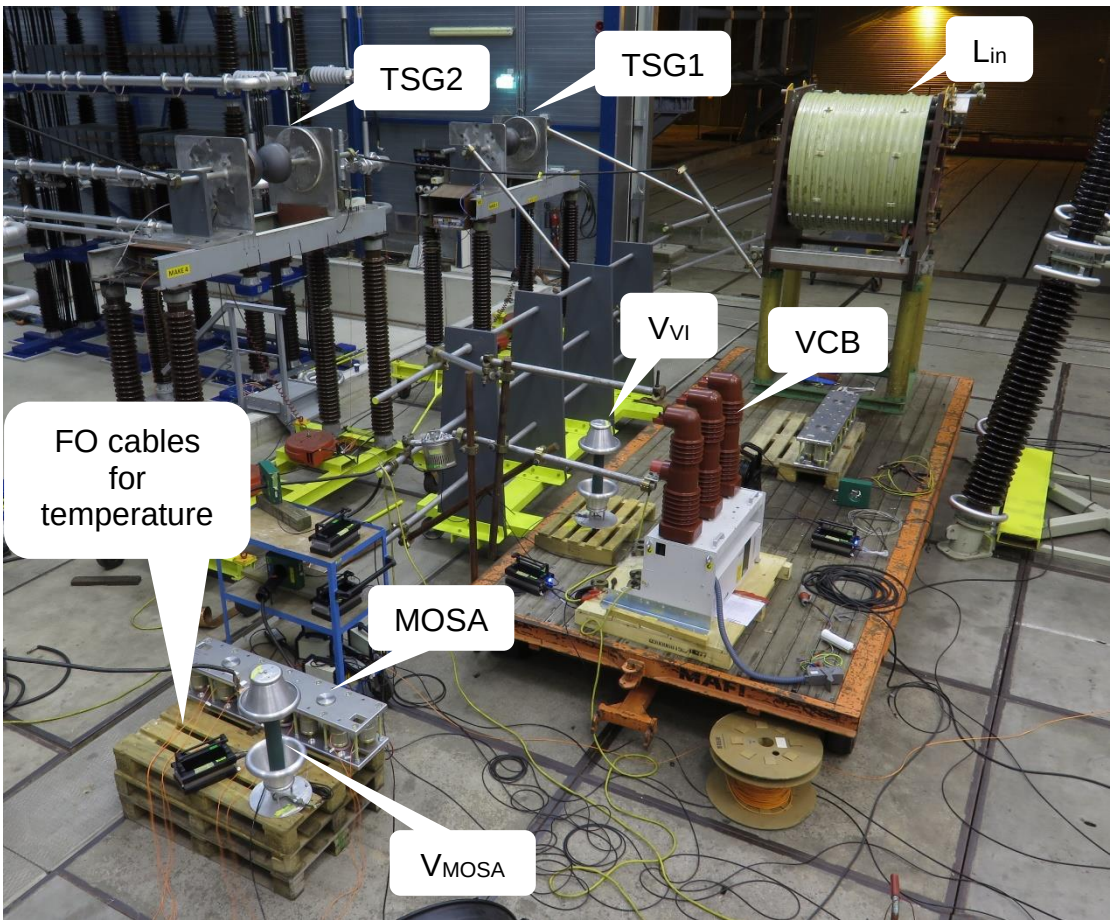

Figure 3-2: Lab set-up of a single break DC CB using VCB Type I

3.1.2.1 TEST DUTY 2 CURRENT INTERRUPTION

Figure 3-3 depicts typical test results of the experimental DC CB shown in the photo above. In this test, the VCB is tripped in advance so that the contacts of the VI separate at time T_1. The detail of the timing sequence is described in Section 2.3. At T_1, the short-circuit current has reached 7.1 kA after which current continues to flow through the vacuum arc. This is shown by red thickened part of the system current shown in Figure 3-3a. Then, 2.9 ms later, a counter current is injected to create CZCs through the VI as shown in Figure 3-3b. It can be seen from this trace that the VI is unable to clear the current at the first 7 CZCs, rather it cleared on the 8th CZC. At each previous CZCs reignition occurred. Considering Figure 3-3c, where the voltage across the VI is plotted, small voltage spikes with alternating polarity are observed at each CZCs. This indicates that the VI is attempting to clear at the CZCs but failed to sustain the initial TIV due to the charge across the injection capacitor. A closer look at the zoomed portion of Figure 3-3c depicts that the magnitude of these voltage spikes at the successive CZCs tend to increase although not monotonically between both polarities. The increase in the reignition voltage at successive CZCs is due to both the increased contact separation and the decreased di/dt caused by the decay in the counter injection current. From the zoomed portion of Figure 3-3b, it can be seen that, due to the superposition of the injection current and the system short-circuit current, the current through the VI oscillates between high

This project has received funding from the European Union's Horizon 2020 research and innovation programme under grant agreement No 691714.

positive value and low negative value (shown by blue circles at local peaks), thus resulting in major loop and minor loop currents between successive CZCs. This seems to have a significant impact on the likelihood of current interruption at a given CZC. Normally, the VI reignition at CZC is caused by thermal and dielectric breakdown with one cause dominating the other depending on the CZC. For example, considering a first CZC (see zoomed plots in Figure 3-3b and c), there is no observable voltage spike unlike for the other CZCs showing that the reignition is mainly caused by thermal effect. This is due to large thermal energy accumulated over the entire arcing duration until the first CZCs. By the time the first CZC is created, the vacuum arc thermal plasma still persists causing it to reignite. At a second CZC, however, a voltage spike of about 2.2 kV can be observed.

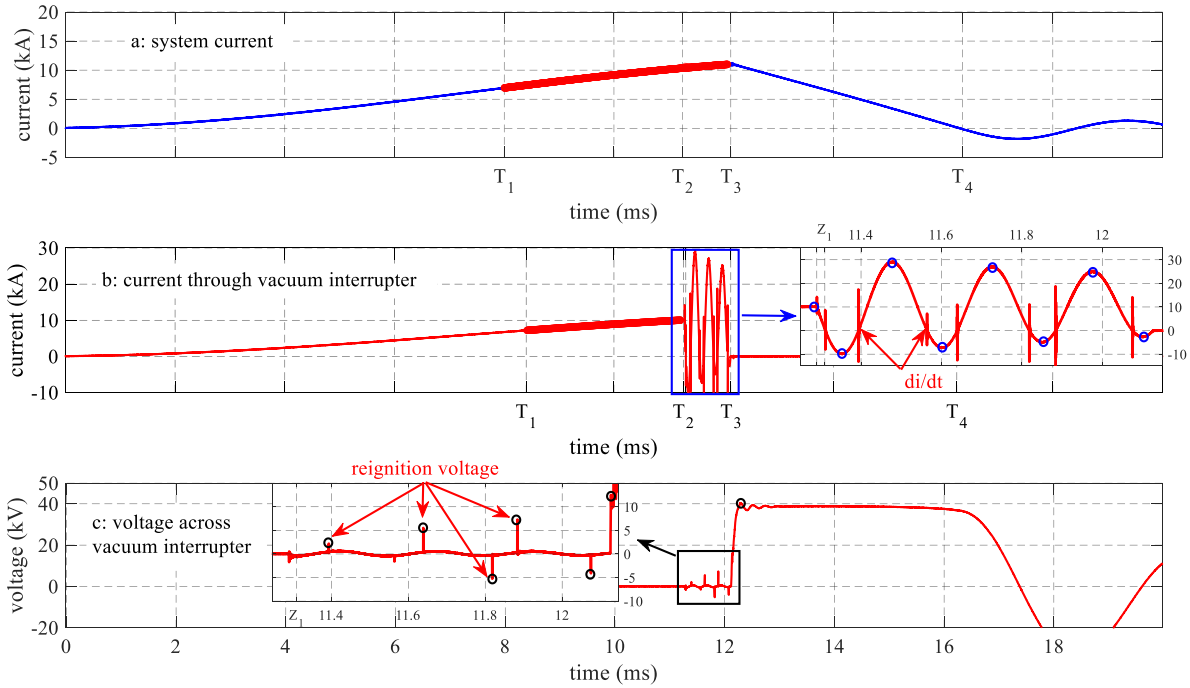

Figure 3-3: Typical test result of experimental DC CB

This means the reignition is caused not only by thermal effect but also slightly by a dielectric effect. Considering the current between the first and second CZCs in the zoomed plot of Figure 3-3b, a minor loop current flows showing limited thermal energy input to the arc burn in this period. On the other hand, between 2nd and 3rd CZCs, a major loop current with peak value of 30 kA and loop duration of 170 µs flows. Thus, the thermal energy input into the arcing gap in this period is high causing thermal reignition at 3rd CZC. There is a small voltage bump observed at this CZC but with lower magnitude than the voltage spike at 2nd CZC despite the contact gap increase. After the 3rd CZC a minor loop current flows until 4th CZC is created. Compared to the previous minor loop, the peak value and the duration of the minor loop in this period is lower, resulting in lower thermal energy injection into the vacuum arc burn in this period. Looking at the voltage plot at 4th CZC, a relatively higher voltage spike (5.5 kV) is seen. This shows the reignition in this case is caused mainly by the dielectric voltage than the thermal energy of metal plasma in the vacuum gap. It must be noted that the dielectric reignition occurred before the full voltage (due to the remaining charge on the injection capacitor) is applied to the gap. In fact, it must be noted

This project has received funding from the European Union's Horizon 2020 research and innovation programme under grant agreement No 691714.

here that the reignition is not caused only by a single factor at a time, but it is showing which factor is more dominant at a given CZC and why.

Proceeding to the 5th CZC, a major loop current flow prior to it. With a similar reasoning as for the 3rd CZC, reignition occurs at this CZC except the reignition voltage is higher in this case. The reignition voltage is almost the same in magnitude as the reignition voltage at the 4th CZC although higher dielectric withstand is expected since the contacts of the VI are still moving apart. Another observation is that as time proceeds, the major loop current peak reduces slightly while its duration increases. The duration increases because of the increased offset caused by a rising system current. On the other hand, the minor loop current peak and duration reduces as the process progresses. This is summarized in Table 4.

Table 4: Parameters near CZCs during current interruption by a VI for example case shown in Figure 3-3

ZC number	1	2	3	4	5	6	7	8
di/dt (A/µS)	498	440	371	365	295	286	209	206
Peak current (kA)	10.1	9.8	29.2	7.2	27.2	5.0	25.3	2.7
Loop duration (µs)	2890[2]	83.7	170	75.2	180	64.1	191	51,3
Voltage across VI (kV)	Negligible	2.2	1.6	5.5	5.26	7.3	4	12.5

Next, a minor loop current with lower magnitude and duration compared to the previous minor loop currents flows between the 5th and before the 6th CZC. At the 6th CZC the VI did not succeed to clear the current. However, a reignition occurred at higher voltage (7.3 kV) across the contact gap, hence justifying dielectric reignition at this CZC. Similarly, next the 3rd major loop current with the longest duration flows until 7th CZC. The 7th reignition occurred at lower reignition voltage (4 kV), lower than at previous three CZCs, due to the presence of more energy into the arc plasma and hence thermal reignition. Finally, current interruption occurred at 8th CZC after a minor loop current flow. Immediately after current interruption, an ITIV of about 12.5 kV is observed across the VI contacts after which it increases (relatively slowly) to the peak value of TIV about 40.4 kV. Note that at all the previous CZCs, the voltage due to the remnant charge in the injection capacitor must be higher than the 12.5 kV observed at the 8th CZC. This is due to some charges lost because of energy dissipation in the inherent resistance of the circuit. Hence, for interruption to have been successful at any of these previous CZCs, the VI should have been able to withstand higher than 12.5 kV voltage.

From the moment of interruption at the 8th CZC and onwards, the short-circuit current is fully commutated to the injection branch of the DC CB. This charges the injection capacitor. The capacitor keeps charging until the protection voltage of the MOSA is reached, thus preventing the VI from higher voltage stress. Henceforth, the MOSA maintains a more or less constant TIV voltage (which appears across the VI, see Figure 3-3c) until the system current is suppressed. Even if thermal energy is no longer injected into the VI contact gap, it must sustain the voltage stress due to the TIV and subsequently the system voltage after current suppression is over.

Nevertheless, it was observed on numerous occasions that the VI fails to withstand the TIV even after local current interruption. Henceforth, this kind of failure is termed as a restrike. Figure 3-4 shows a test result in which a

[2] arcing duration from contact separation till 1st ZC

This project has received funding from the European Union's Horizon 2020 research and innovation programme under grant agreement No 691714.

restrike occurred before the injection capacitor is fully charged to the protection level of the MOSA. First, the VI arc is allowed to burn for about 3.92 ms before the injection circuit triggered spark gap (TSG2) is fired to inject a counter current, see thickened red trace in Figure 3-4a. Compared to the test result shown in Figure 3-3, the VI's arcing duration is prolonged by 1 ms in this case. It is important to note that even though an increase in the arcing duration typically does not lead to current interruption at earlier CZCs, in this case the VI cleared at the 6th CZC. The interruption process follows a similar behaviour as for test result shown in Figure 3-3. The parameters near current zero are provided in Table 5. From the results shown in Figure 3-4, the VI (dielectrically) breaks down (restrikes) 70 µs after local current interruption. Note that the restrike occurs while the TIV is rising (before the peak value is reached) as the injection capacitor is being charged by the system current.

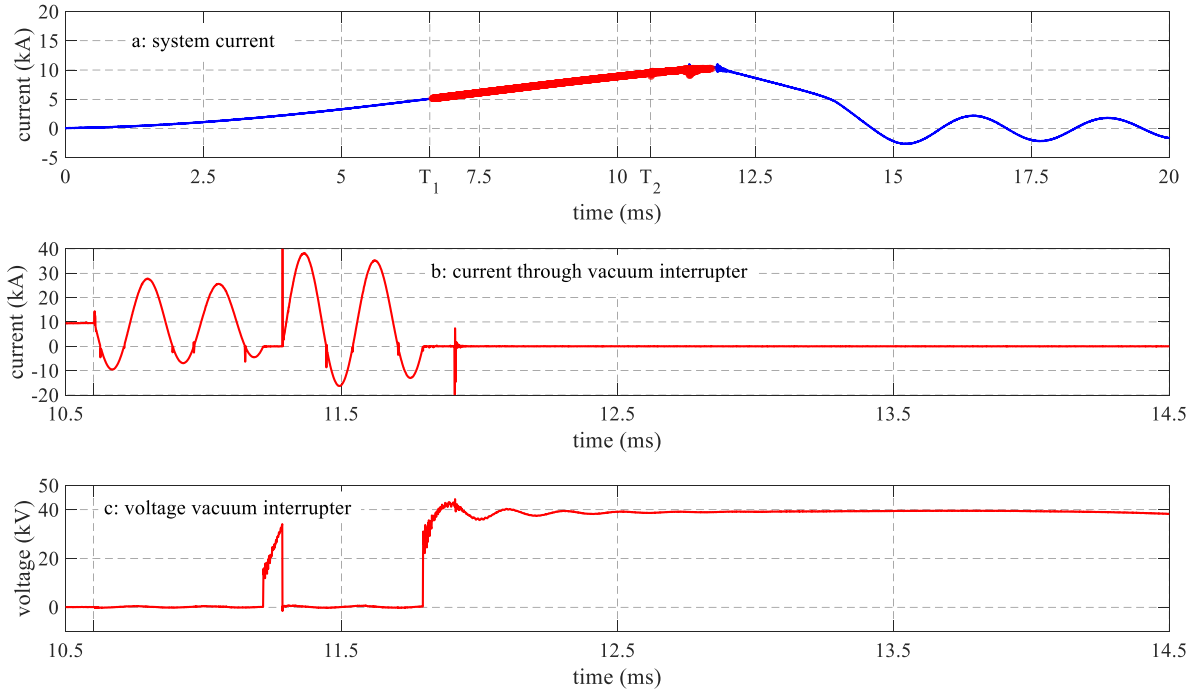

Figure 3-4: Example case test result showing restrike of VI

Following the restrike, another string of current oscillation through the VI is observed. Since at the restrike the injection capacitor is charged to a higher voltage than its pre-charge level, the magnitude of the injection current and hence the current through the VI is higher than the oscillation before the restrike. As a result, the parameters near current zero change, for example, di/dt near CZC is increased by almost 50 % in this case and so are the peak values of the loop currents (see Table 5). At this point, the VI contacts are still moving apart, resulting in a slight successive increase in dielectric strength with each CZC. Hence, after a restrike, the current interruption occurred a few CZCs later at a higher di/dt compared to the current interruption before the restrike. In fact, in both cases, interruption happened after a minor loop current. It must be noted that from the system point of view, the oscillating current through the VI is not observable. The system does not see whether the VI cleared on 1st CZC or not. The system current continues to rise until the VI clears, resulting in a slightly higher peak current than expected. This has an impact on the energy absorption of the MOSA as well.

This project has received funding from the European Union's Horizon 2020 research and innovation programme under grant agreement No 691714.

Table 5: Current zero parameters for the example test case shown in Figure 3-4

ZC number	1	2	3	4	5	6	7	8	9	10
di/dt (A/µS)	420	412	338	335	262	256	613	603	527	513
Peak current (kA)	9.6	9.5	27.7	6.9	25.6	4.5	38.3	16.3	35.1	13
Loop duration (µs)	3920[3]	86.5	174	77.6	186	65.6	158	96.8	164	90.4
Voltage across VI (kV)	Negl.	7.85.	Negl.	4.5	Negl.	3.75	Negl.	Negl.	Negl.	2.2

Due to the inherent behaviour of the VI, a restrike(s) may occur at a later stage even after sustaining the peak TIV for some time. Figure 3-5 depicts a typical test result in which a restrike occurred during the current suppression phase. Similar phenomena as for the previously discussed test cases, such as reignition voltage spikes at CZCs following minor loop current, are observed. Current interruption occurred at the 10th CZC in this case. The parameters near CZCs including the CZCs after the restrike are shown in Table 6.

With a similar reasoning as for the example case shown in Figure 3-4, the oscillating current after the occurrence of a restrike has a higher magnitude than before the restrike. Normally, the TIV at this point is 50% higher than the pre-charge voltage (the pre-charge voltage is assumed to be equal to the system voltage). Hence, the parameters near CZCs including the di/dt and the peak value of the loop currents are also increased by 50 % compared to the corresponding values before the restrike. As can be seen from Figure 3-5, the restrike happened about 1.2 ms after local current interruption. During this time, the system current has been suppressed by about 3 kA from its peak value. After the restrike the system current starts to rise again although the VI clears before the system current exceeds the previous peak value. However, this is not always the case and the VI may even be unable to clear after the restrike which has also been observed during the test campaign. The main impact of a restrike in this case is a longer total current interruption period and an increased energy absorption in the MOSA. The occurrence of a restrike hence also has an impact on the system.

Moreover, the local current interruptions (both before and after the restrike) occurred after minor loop currents. For the VCB discussed in this section, in fact, there are only few cases where interruption occurred on the first CZC or after the major current loop. For example, among 98 of the 1st CZ attempts only 6 times the VI could interrupt. Statistical analysis of the test results is presented in Section 3.3.

[3] arcing duration until 1st ZC

This project has received funding from the European Union's Horizon 2020 research and innovation programme under grant agreement No 691714.

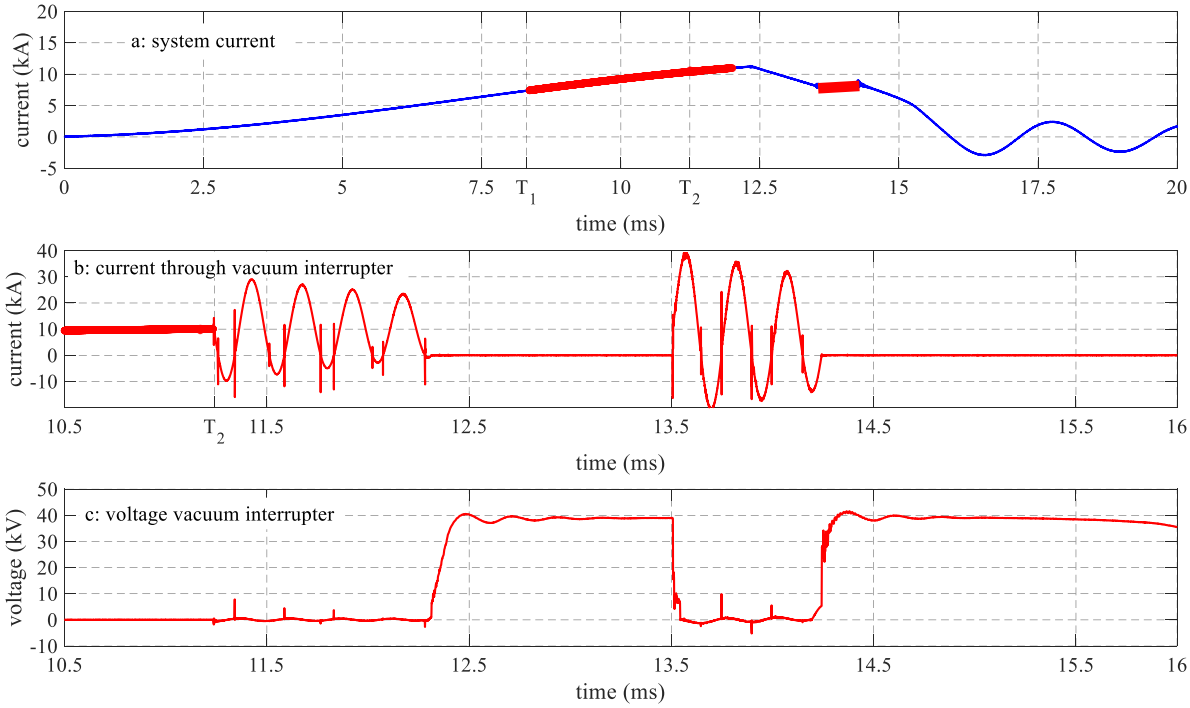

Figure 3-5: Example case test result where VI restrikes on steady state TIV

Table 6: Parameters near current zero for the example test case shown in Figure 3-5: Example case test result where VI restrikes on steady state TIV

ZC number	1	2	3	4	5	6	7	8	9	10	1	2	3	4	5	6
di/dt (A/µS)	454	437	377	363	298	286	215	212	116	110	740	692	639	592	542	507
Peak current (kA)	10.1	9.8	29.0	7.3	26.8	4.9	25.0	2.9	23.4	0.9	38.5	20.5	35.5	17.5	31.5	13.8
Loop duration (µs)	2970[4]	82.3	171	75.8	178	65.4	191	52.3	208	30.1	140	102	150	98.2	153	94.7
Voltage across VI (kV)	N[5]	7.843	N	4.486	1.42	3.735	N	N	2.7	6.592	2.4	9.872	5.2	5.55	N	27.98

[4] arcing duration until 1st ZC
[5] Negligible

This project has received funding from the European Union's Horizon 2020 research and innovation programme under grant agreement No 691714.

3.1.2.2 TEST DUTY 1 CURRENT INTERRUPTION

The performance of VIs depends on the magnitude of current to interrupt. Figure 3-6 shows low current (2.3 kA) interruption by a VI. For the test case shown in the figure, the VI arcing duration is 4 ms. The parameters of the injection circuit remain the same as for the example cases discussed above. Thus, counter current with peak value of 20 kA at a frequency of 4 kHz is injected. At a low current of 2.3 kA, an injection current of such a peak magnitude is not needed to create CZCs. However, in practical operation, the injection current remains the same despite the magnitude of the interruption current and this is the motivation for keeping the same injection circuit under different interruption current levels.

As mentioned earlier, given counter injection current peak value and frequency, the parameters near CZCs depend on the magnitude of interruption current. For example, the di/dt, the minor loop current peaks and durations are higher while the major loops current peak and duration are lower compared to when interrupting high current, see Table 7. A more striking difference, in addition to increase in di/dt, is the initial TIV at CZCs. The full ITIV may not be observed at reignited CZCs. The higher initial TIV is due to significant proportion of charge remaining on the injection capacitor since only slight discharge is needed to create CZ when interrupting low current. Thus, compared higher current interruption cases where the thermal reignition plays a major role, for low current interruption, the increased di/dt and initial TIV play a major role whether a reignition occurs at a CZC.

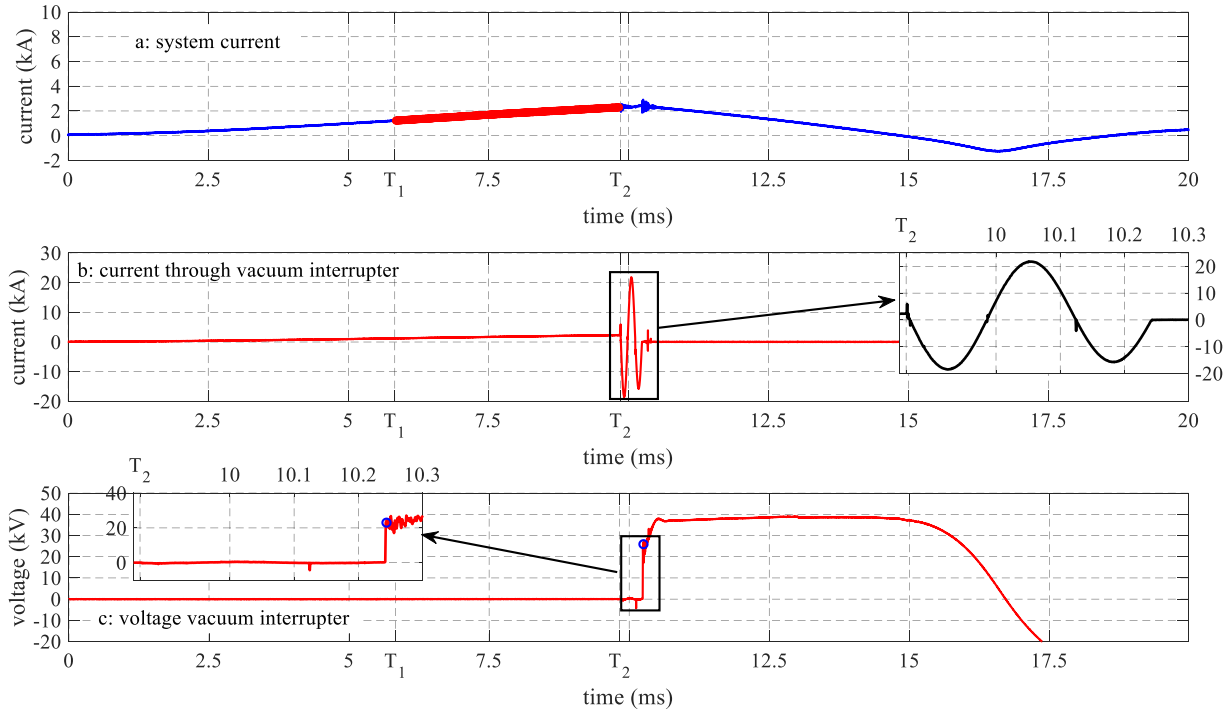

Figure 3-6: Example test case showing low current interruption

During the test campaign (for the VI under discussion), low current interruption was repeated 10 times and in no occasion current interruption occurred at 1st CZC. From Figure 3-6, it can be seen that the local current interruption is achieved at 4th current zero.

This project has received funding from the European Union's Horizon 2020 research and innovation programme under grant agreement No 691714.

Most of the current interruptions occurred at 4th current zero although in a few cases interruptions occurred at 2nd and 6th CZCs and in all cases after minor loop current.

Due to the V-I characteristics of the MOSA, the TIV during current suppression is lower in this case compared to when interrupting the higher current test duties. This has an impact on the duration of current suppression period. With the increased impedance (to limit current) while keeping all other test circuit parameters, the reduced TIV results in the same duration of current suppression period as for higher current test duties, see Figure 3-6.

Table 7: Parameters near current zero for the example test case shown in Figure 3-6.

ZC number	1	2	3	4
di/dt (A/µS)	516	502	470	432
Peak current (kA)	2.32	18.5	21.9	15.8
Loop duration (µs)	4010 (arcing duration until 1st ZC)	120	139	118
Voltage across VI (kV)	Negl.	Negl.	4.3	23

3.1.2.3 TEST DUTY 3 CURRENT INTERRUPTION

Among all the tests the high-current test duty (16 kA) is the most challenging for the VI as most of the failures were recorded during this test duty. There are number of reasons for this. First of all, the number of CZCs that can be created (with the designed injection circuit) at this test duty current is limited, a maximum of 4 CZCs, thus excluding the chance of current interruption if a reignition occurred at 4th CZC.

Figure 3-7 shows a high-test duty current (15.5 kA) interruption by a VI. The vacuum gap is allowed to arc for 3.96 ms before the counter current is injected as shown by the red, thickened trace shown in Figure 3-7c. Due to the high thermal energy input to the vacuum arc, no interruption at the 1st CZCs is observed. In a few cases interruption occurred at the 2nd CZC. In the example test case shown in Figure 3-7, the VI attempts to clear at the 2nd CZC where reignition occurred due to the ITIV of about 19 kV. In this case, the VI could sustain the voltage until the entire ITIV is applied. There is no observable interruption attempt by the VI on the 3rd CZC mainly due to high thermal energy following the major loop current of 35 kA peak and 200 µs duration, see Table 8. Current interruption occurred at 4th current zero following a minor loop current of 2.4 kA and about 42 µs duration. The ITIV observed at this CZC is 14.3 kV and the VI could withstand it. Following local current interruption, the capacitor keeps charging up to the peak TIV of 45 kV. Another observation is that at CZCs of high current test duty, the di/dt is lower, see Table 8.

This project has received funding from the European Union's Horizon 2020 research and innovation programme under grant agreement No 691714.

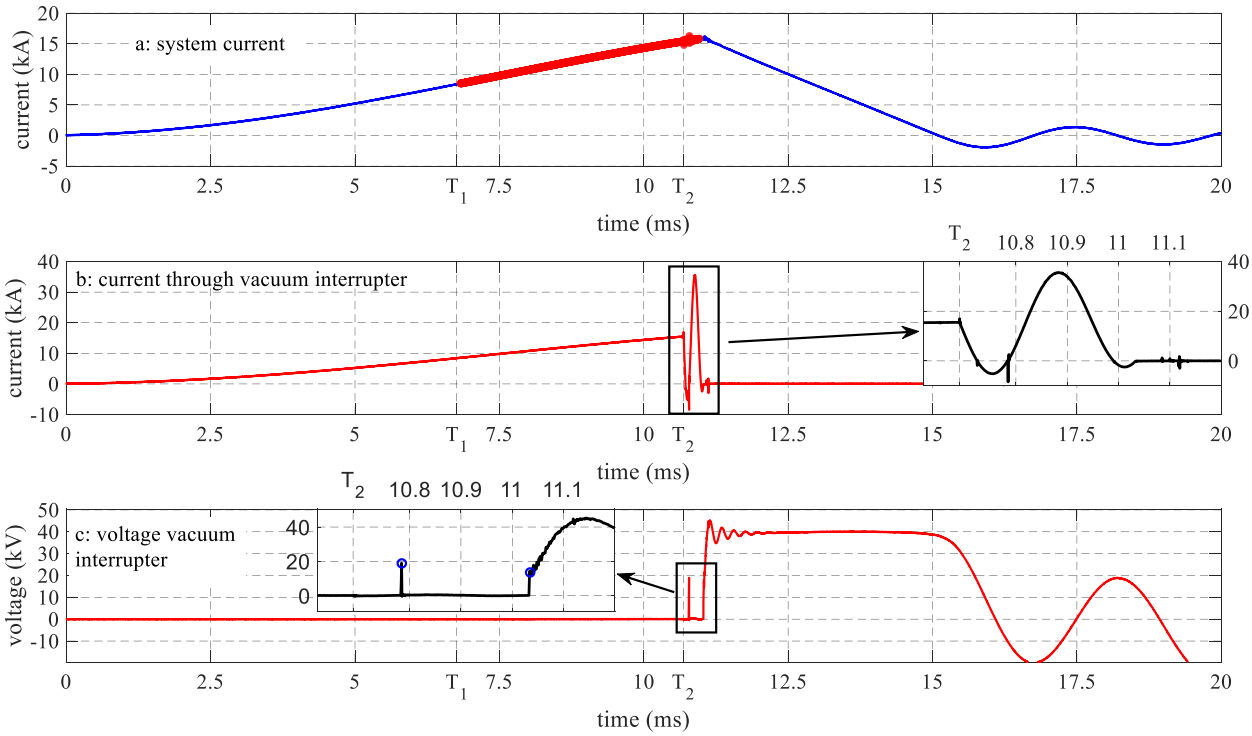

Figure 3-7: Example case test result showing high test duty current interruption

Table 8: parameters near current zero for the example test case shown in Figure 3-7

ZC number	1	2	3	4
di/dt (A/µS)	285	283	211	211
Peak current (kA)	15.6	5.18	35.4	2.4
Loop duration (µs)	4010 (arcing duration until 1st ZC)	59.2	207	41.6
Voltage across VI (kV)	Negl.	18.9	Negl.	14.3

The same test is repeated 10 times and in about 40 % of the cases it failed to interrupt. Figure 3-8 shows a failure to interrupt case. Here, the arcing duration until current injection is set to 3 ms. It can be seen from the voltage plot that the VI attempts to clear at the 2nd and 4th CZCs where dielectric reignition occurred. At these CZCs, reignitions occurred at 6.4 kV and 10.4 kV, respectively. The parameters near CZCs for this test are provided in Table 9. These parameters are very similar to the test case shown in Figure 3-7 except the arcing duration until the 1st CZC which is shorter in this case. After 4th CZC, there is no other chance for the VI to clear as there is no CZC and hence, the VI continues to arc until the test circuit takes protective action.

This project has received funding from the European Union's Horizon 2020 research and innovation programme under grant agreement No 691714.

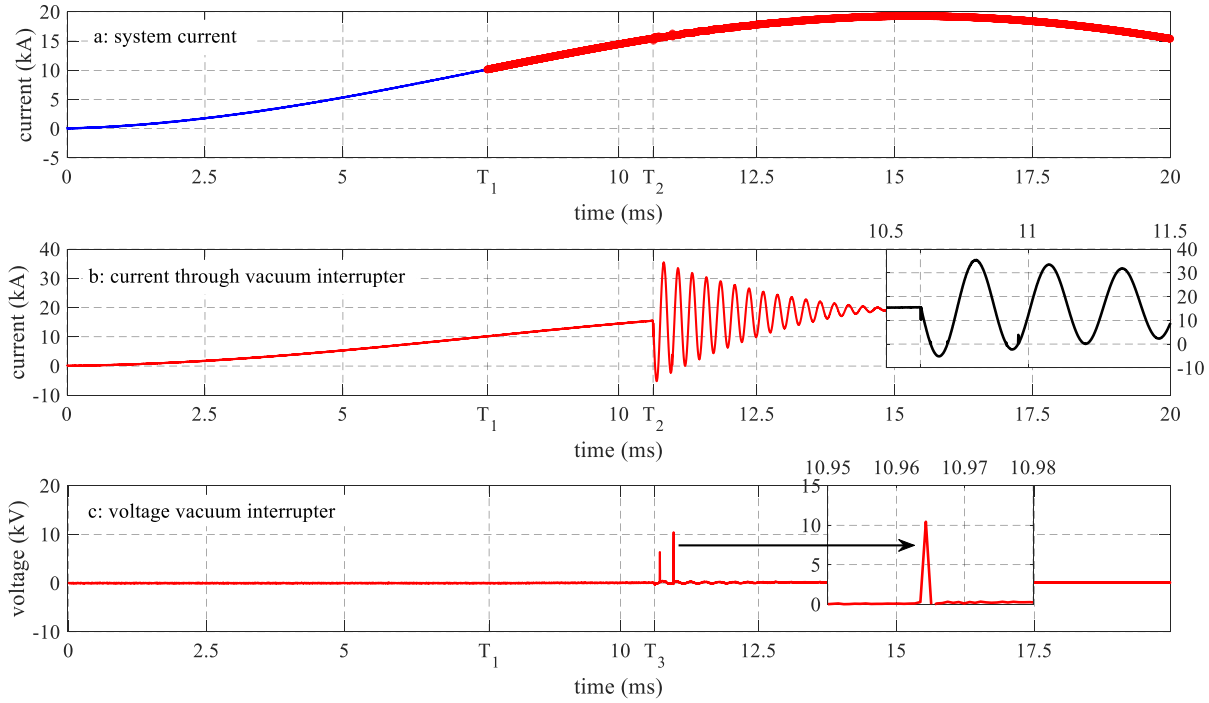

Figure 3-8: Example case showing failed current interruption

Table 9: Parameters near current zero for the example test case shown in Figure 3-8

ZC number	1	2	3	4
di/dt (A/µS)	340	322	244.5	210
Peak current (kA)	15.6	5.19	35.4	2.3
Loop duration (µs)	3050 (arcing duration until 1st ZC)	57.6	208	41.6
Voltage across VI (kV)	Negligible	6.4	Negligible	10.4

Tests have been performed at shorter arcing times for the VI discussed in this section, but it could not succeed to interrupt. Even at longer arcing durations (4 and 5 ms) several failure cases have been recorded showing the limit of the VI to interrupt high current.

3.1.3 TEST RESULTS ANALYSIS OF DOUBLE INTERRUPTER EXPERIMENTAL DC CB – VCB TYPE A

Due to inherent behaviour of VIs, increasing the gap length does not increase performance linearly. More specifically, the voltage withstand capability does not scale linearly with gap distance. In fact, a linear relationship is valid only for the first few millimetres (1-2 mm) after which the dielectric withstand does not grow even if the gap length is increased. Otherwise, in order to maintain the linear relationship over a long gap length, bulky contact surfaces are needed which lead to uneconomical design. An alternative way of increasing the dielectric strength of VI based circuit breakers is to use a series connection of VIs. Based on this, a double interrupter DC CB, where two VIs are connected in series, is set up in a test laboratory to investigate the performance at high voltage application. In order to compare the performance with a single interrupter case, the double interrupter DC CB is designed with the intention that the parameters near CZCs are kept the same per VI. For example, the counter

This project has received funding from the European Union's Horizon 2020 research and innovation programme under grant agreement No 691714.

injection current peak magnitude and frequency are the same as for the single interrupter case while the charging voltage of the injection capacitor is doubled. The injection capacitor and inductor are modified accordingly. The parameters of the injection circuit are shown in Table 3 in Chapter 2. However, the test duty current magnitudes and the corresponding rates-of-rise remain unchanged while the supply voltage and test circuit impedance are doubled compared to single interrupter case.

Figure 3-9 shows the photo of the test set-up of the double interrupter experimental DC CB in the test laboratory. Two MOSA stacks are used in series to double the clamping voltage of the TIV across the two VIs. For the purpose of performing a large number of tests without over-heating the MOSAs, two sets are used in parallel (for energy sharing), although this results in a slightly reduced TIV. A very critical aspect when using VIs in series (especially when using a common injection branch) is the voltage distribution. It is necessary to ensure equal voltage sharing among the two VIs in this case. For this purpose, grading capacitors are connected to each VI as shown in the figure.

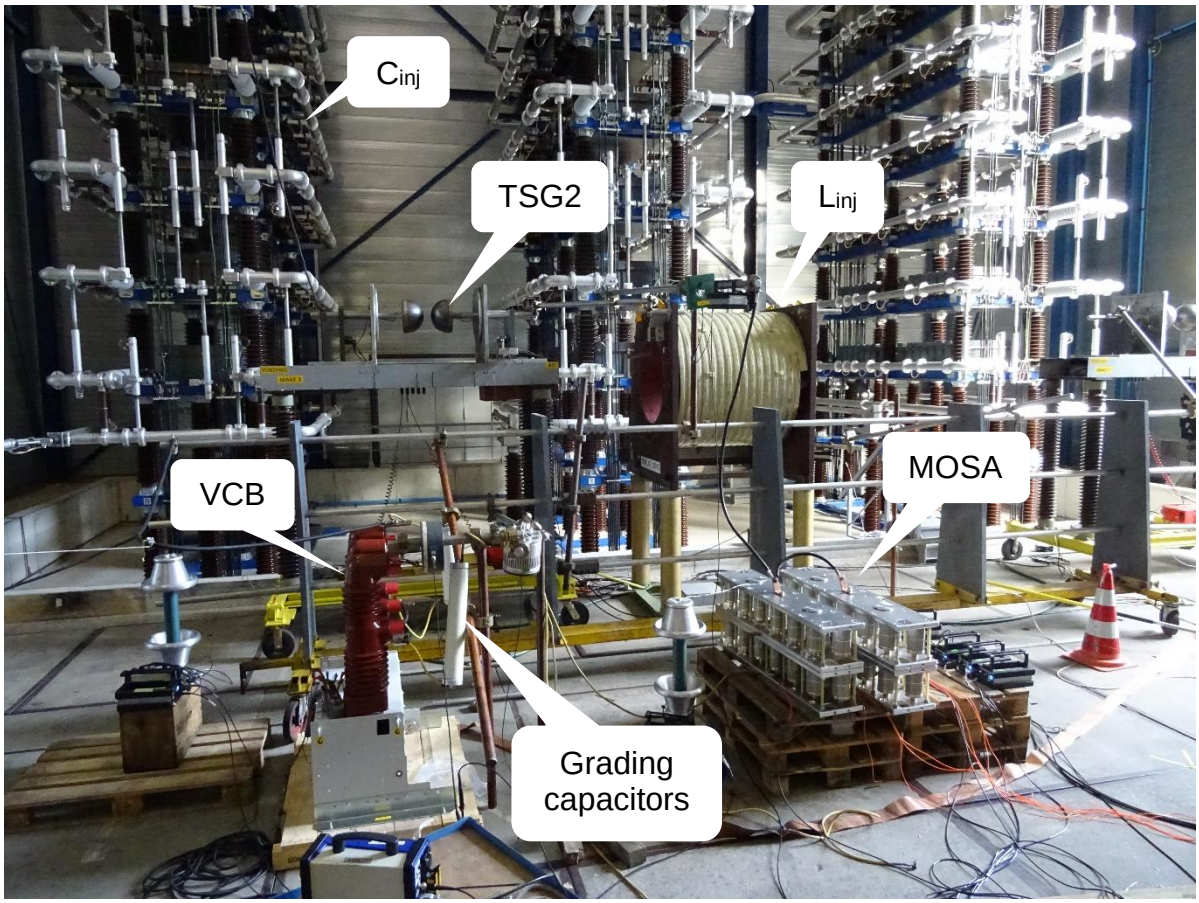

Figure 3-9: Laboratory set-up of double interrupter experimental DC CB using VCB Type I

In the experimental test campaign, grading capacitors of 700 pF and 2500 pF are used. Nevertheless, the circuit is designed to achieve a similar di/dt through each VI at CZCs, and ideally, similar initial TIV at CZCs. However, the latter is practically challenging to achieve, and this is discussed below.

This project has received funding from the European Union's Horizon 2020 research and innovation programme under grant agreement No 691714.

In any case, it is necessary that both VI contacts are open by the time CZC is created. That is to ensure both the VIs have the chance to clear at the same time. Otherwise, only one of the two VIs carry the entire intended TIV burden. However, practically there are some cases where only one VI clears while the other does not and hence the entire TIV appears across one VI.

Figure 3-10 shows an example test case result by a double interrupter set-up shown in Figure 3-10 . The arcing duration until the moment of current injection is 4 ms in this case, see the thickened red trace in Figure 3-10a. The current interruption occurred on the 2nd CZC following minor loop current. A very interesting observation is, however, on the voltage measurement shown in Figure 3-10b. The black trace shows voltage measurement across both interrupters (although the voltage divider is placed a few meters away, and hence there is some induced oscillation observed) whereas the red trace shows the voltage measurement across one of the two VIs.

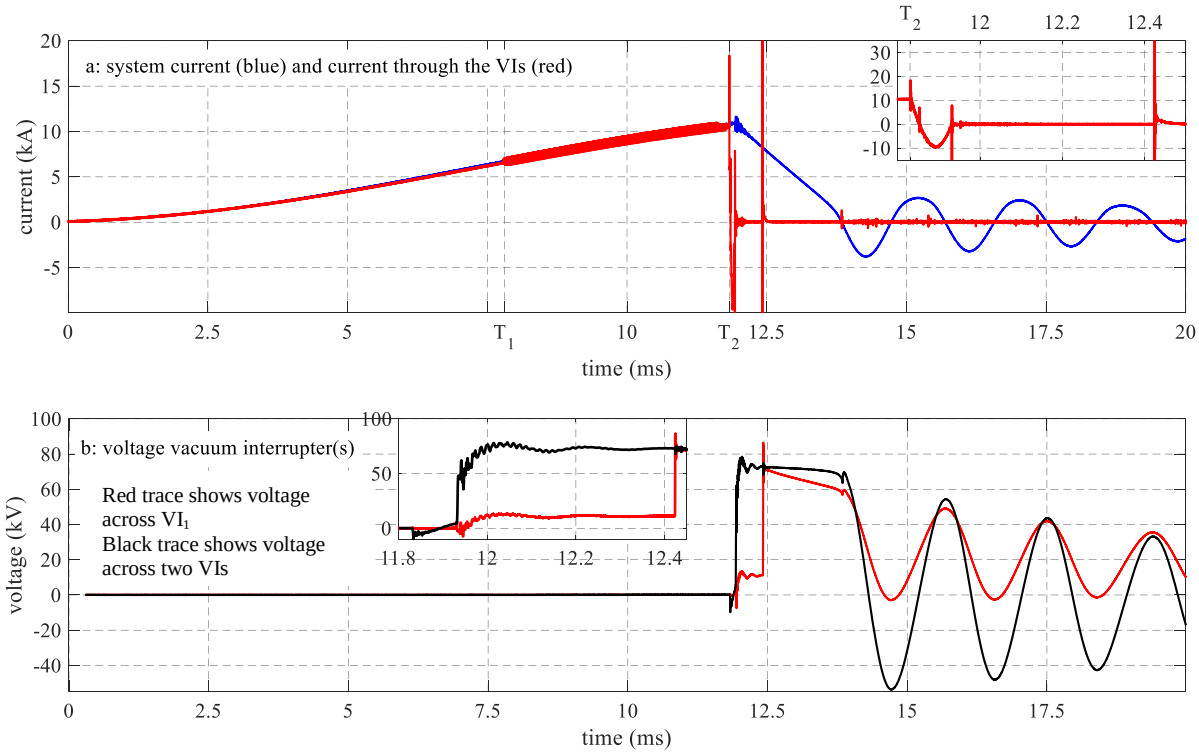

Figure 3-10: Example case test result by double interrupter experimental DC CB

From the voltage plots of this figure it can be seen that only one interrupter cleared on the 2nd CZC. The total ITIV measured across the two VIs is 46 kV whereas only about 6 kV followed by some transients is observed on the measurement shown by the red trace. The transient observed is due to reignition in the VI across which the voltage measurement is placed (call this VI_1 for convenience). Hence, only VI_2 cleared in this case and had to withstand the entire ITIV and the TIV afterwards. Because of the current interruption in the VI_2, there is no current flow in the other VI leading to dielectric recovery in the latter. As a result, although the voltage is never redistributed equally, there is a slightly increased voltage across VI_1. Nevertheless, for about 0.5 ms, more than 85% of the TIV is applied across only VI_2 after which a restrike occurs, just before the 12.5 ms mark on the graph. However, the restrike of VI_2 did not lead to resumption of the system current flow in the VIs and another set of current injection oscillation as in the single interrupter case. This is because when VI_2 restrikes, the TIV is redistributed to VI_1 as can be seen by the huge jump in the red trace, equalling the total TIV momentarily. The transient observed in the

PROMOTiON – Progress on Meshed HVDC Offshore Transmission Networks

This project has received funding from the European Union's Horizon 2020 research and innovation programme under grant agreement No 691714.

red trace just before the 12.5 ms mark in Figure 3-10a is due to the discharge of the grading as well as stray capacitors. In this case a test is deemed as successful because the measurements and the interruption process seen from outside the breaker are normal although it might have taken longer. Note that the duration of the current suppression time is rather short in this case and VI_1 sustained the TIV only for about 1.5 ms. This does not guarantee successful interruption in case the current suppression period in a real application is longer and also taking into account that the nominal DC voltage is applied immediately after current suppression.

A closer look at the test results from the double interrupter DC CB shows that in most of the cases the two VIs do not clear at the same CZC and hence, the voltage distribution is never equal even if 700 pF grading capacitors are used. Only in a few cases, both VIs clear at the same CZC and in such a case the voltage distribution is better. This is shown in Figure 3-11 where the ITIV is more or less equally distributed. In addition, due to stray capacitances to ground, the VI on the high potential side is found to be carrying the higher proportion of the TIV.

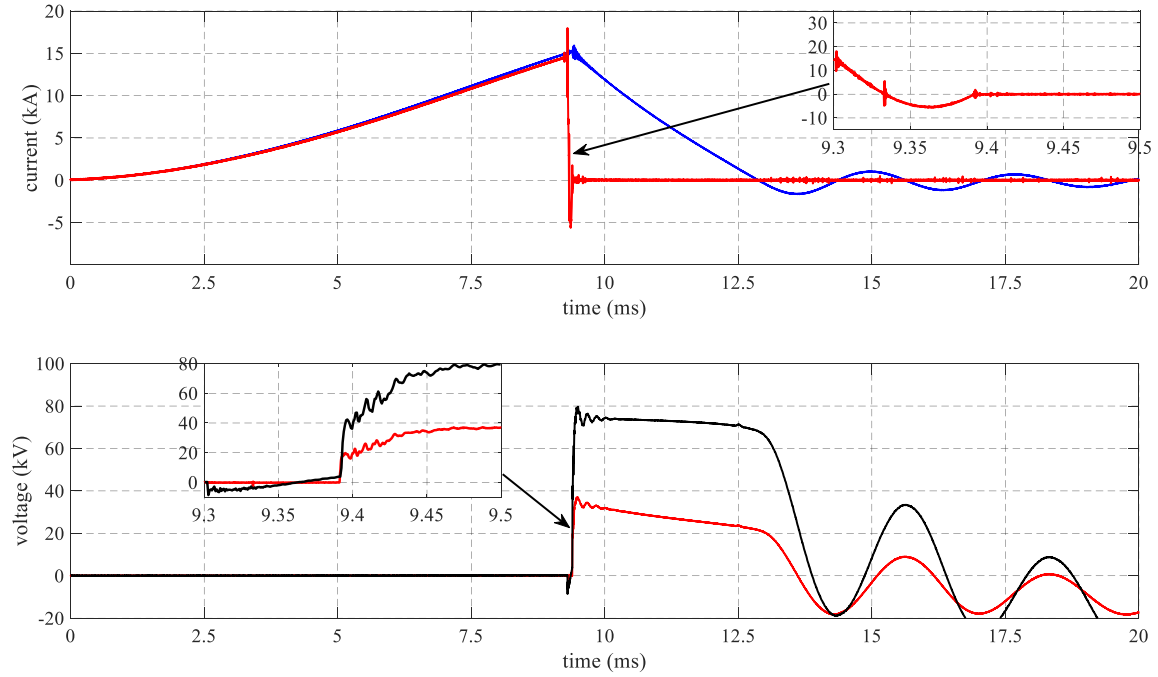

Figure 3-11: 16 kA current interruption by double break experimental DC CB – typical voltage sharing issue

Figure 3-12 shows typical test result in which the impact of non-simultaneous clearing by series connected VIs and hence, unequal TIV sharing is observed. In this case VI_1 cleared on 2nd CZC while VI_2 did not, as observed from the voltage traces. The entire TIV is seen across VI_1. About 47.2 µs later a restrike occurred in VI_1. However, with a similar reasoning as in the example shown Figure 3-10, VI_2 could take over the TIV from the VI_1.

In this case the VI_2 could not sustain the TIV for a long duration and it restrikes about 58 µs later. At this time, the VI_1 has recovered its dielectric strength and hence, could take over the TIV back. In the meantime, the TIV is rising as can be observed from the zoomed part of Figure 3-12b. However, this time the VI_1 sustained the TIV for a very short duration (12 µs) after which it restrikes for the second time. At this stage the VI_2 is dielectrically not ready to withstand the TIV and as result the system current flow re-establishes through both VIs with the superimposed discharge from the injection capacitor. With a similar reasoning as for a single interrupter case, the peak magnitude and duration of the oscillating current through the VIs is increased by about 50 %. After 8 CZCs

This project has received funding from the European Union's Horizon 2020 research and innovation programme under grant agreement No 691714.

current interruption occurred but only VI_2 cleared in this case. This can be observed from the voltage traces shown Figure 3-12b.

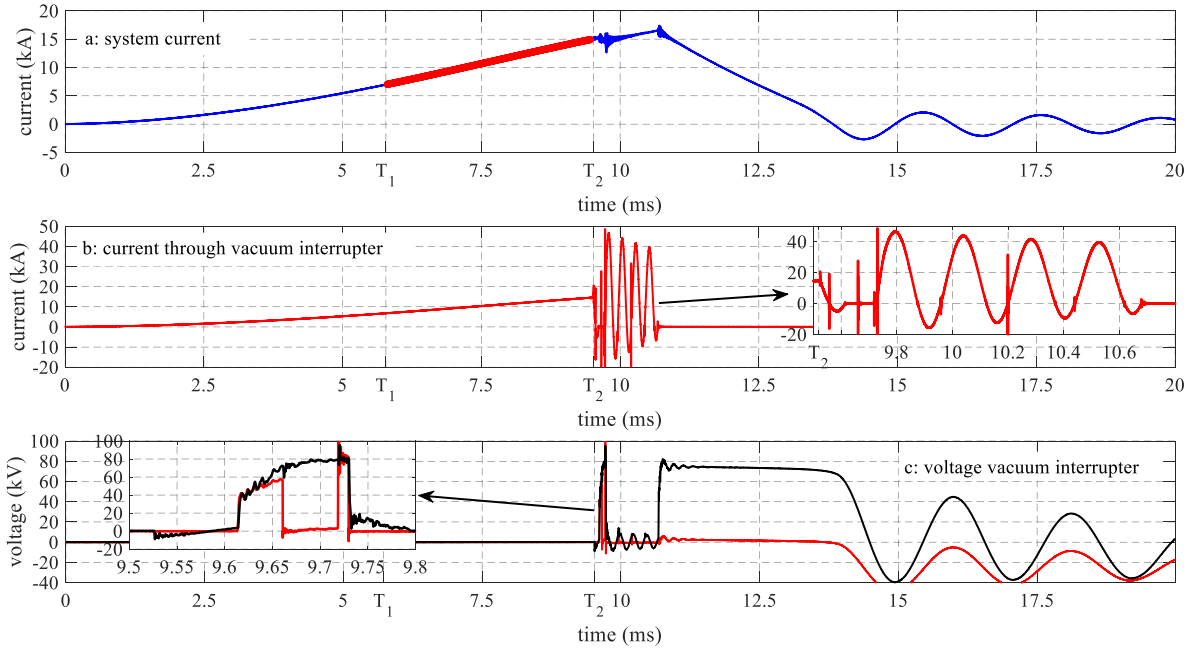

Figure 3-12: 16 kA current interruption by experimental DC CB – Typical voltage sharing issue

A very similar situation as the example discussed in Figure 3-12 is observed during test duty 2 (10 kA) current interruption as depicted in Figure 3-13. In this case the VI_1 cleared at 10th CZC and could withstand the TIV for about 200 µs after which a restrike occurred. Then VI_2 could take over the TIV for about 33 µs after which it re-struck. After VI_2 re-struck, both VI could not clear the current even if 18 CZCs were created.

PROMOTiON – Progress on Meshed HVDC Offshore Transmission Networks

This project has received funding from the European Union's Horizon 2020 research and innovation programme under grant agreement No 691714.

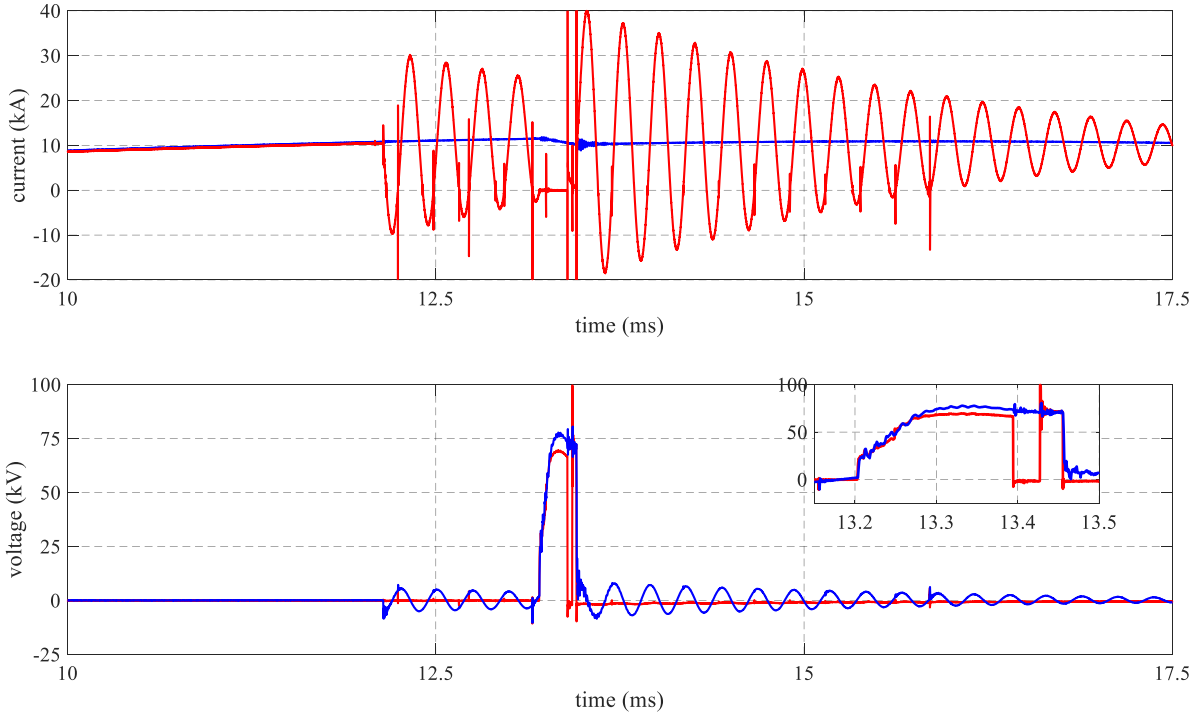

Figure 3-13: Example case test result showing failure to interrupt test duty 2 (10 kA) current after restrike by double interrupter DCCB

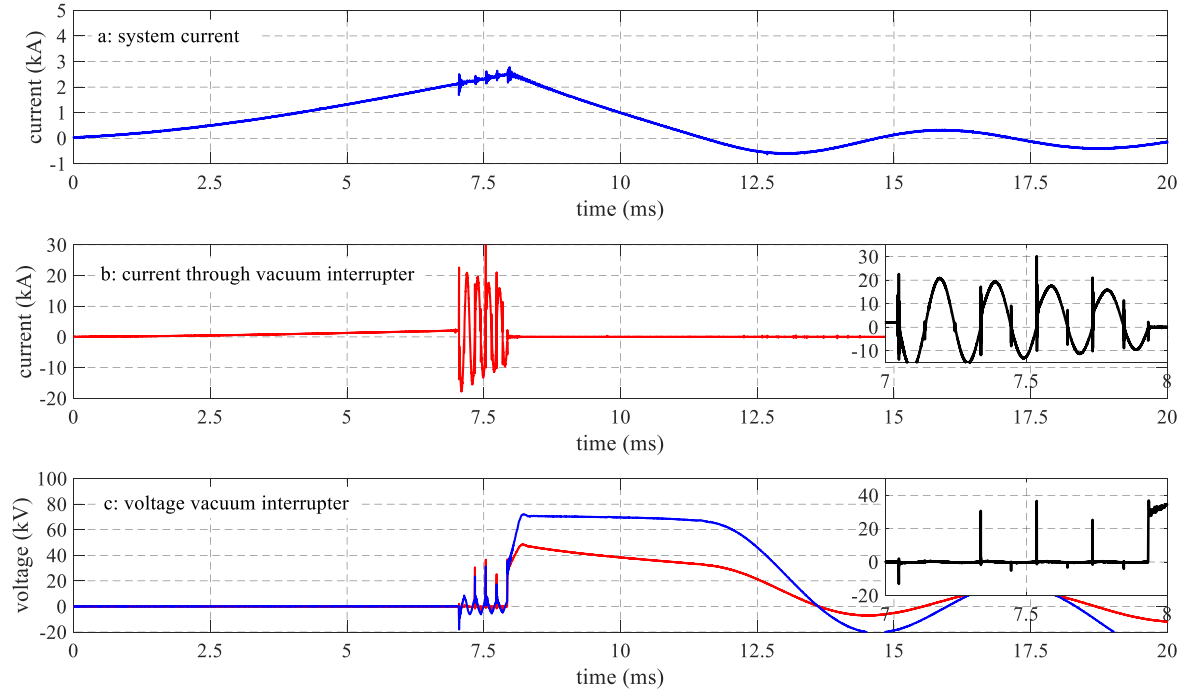

Figure 3-14: Example case showing low current interruption by double interrupter experimental DC CB

Figure 3-14 shows low current (2 kA) interruption by double interrupter experimental DC CB. In this case it took about 10 CZCs to clear the DC current after which only VI_1 cleared. It is only VI_1 which cleared because the entire ITIV is measured across VI_1 although there is redistribution when the capacitor starts charging. From the zoomed

This project has received funding from the European Union's Horizon 2020 research and innovation programme under grant agreement No 691714.

section in Figure 3-14c, it can be seen the VIs indeed attempted to clear at earlier CZCs. Especially the attempts following minor loop currents are quite visible from the reignition voltage. Although only VI_1 sustained the entire ITIV (37 kV), the VI_2 could also share about 33 % of the TIV afterwards. Similar to the single interrupter test cases, tests have been repeated a number of times and in none of the cases it cleared on the 1st CZCs.

3.1.4 STATISTICAL DATA OF TEST RESULTS OF VCB TYPE A

Figure 3-15 shows the distribution of current interruptions against the number of CZC for all tests done on a particular type of VCB. This data combines test results for both single interrupter and double interrupter cases using VCB type A. Of the total of 98 tests performed, only in 6.1 % of the tests could it clear at the 1st CZC. The performance increases at the 2nd CZC to 25 % of the remaining 92 tests (since in 6 tests cleared at 1st CZC). The proportion of successful current interruptions at the 3rd CZC drops significantly to less than 3 %. This is because the 3rd CZC occurs after a major loop current flow. In general, it is clear from this graph that most of the current interruptions occurred at even numbered CZCs which occur after minor loop current flow.

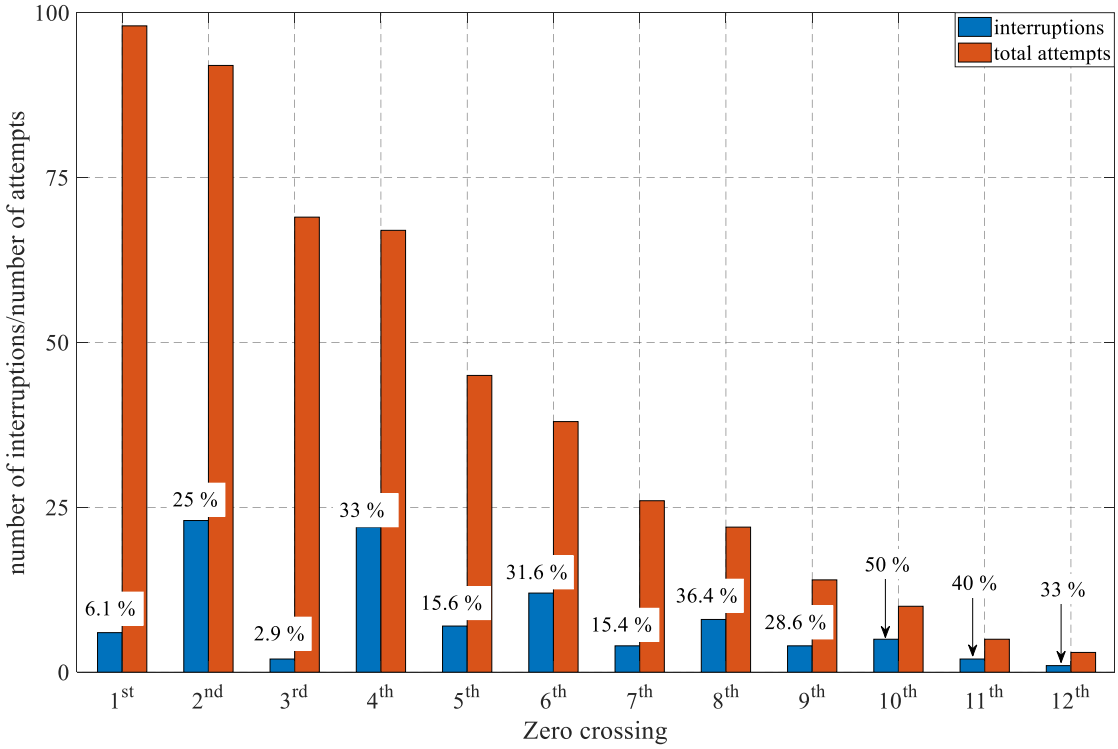

Figure 3-15: Proportion of current interruption at a given current zero

Figure 3-16 shows the rate-of-change of current (di/dt) at a given CZC versus the peak value of current just before the same CZC both at current interruptions as well as reignitions. Looking at the x-axis which shows the current peak magnitude before CZC, two regions can be observed, below and above the 20 kA value. Most of the interruptions occurred when the peak current just before CZC is below 20 kA. Considering the region above 20 kA, there are a few cases where the VI failed to clear even if the di/dt is very small.

PROMOTiON – Progress on Meshed HVDC Offshore Transmission Networks

This project has received funding from the European Union's Horizon 2020 research and innovation programme under grant agreement No 691714.

Another important observation is the impact of di/dt on the current interruption performance. It can be seen from Figure 3-16 that in no circumstance the VI could clear for di/dt higher than 620 A/µs although much higher di/dt could be created at specific CZC with very low peak loop current. Although the arc time constant of a vacuum interrupter is very short, there is a limit to it. The vacuum arc can cool from several hundreds of degree Celsius to ambient within microseconds. However, when current zero is created before the arc cools down, then reignition occurs.

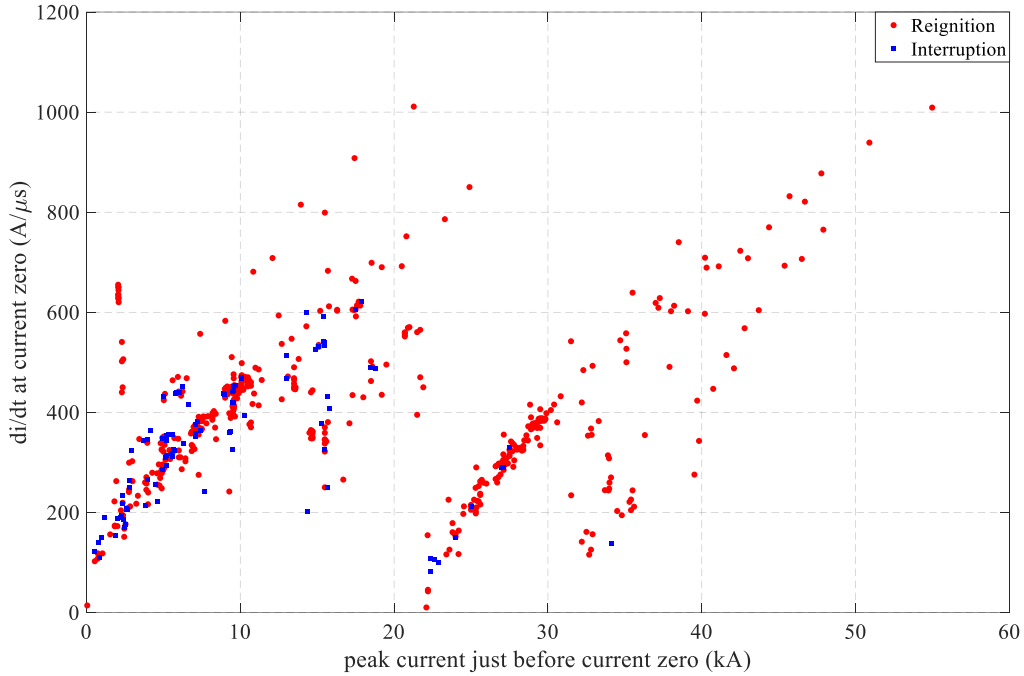

Figure 3-16: current interruption in VCB Type A as a function of rate-of-change of current at current zero and current magnitude prior to current zero

3.1.5 TEST RESULTS ANALYSIS OF SINGLE INTERRUPTER EXPERIMENTAL DC CB – VCB TYPE B

In order to investigate the impact of the differences in the design of VI contacts, the experimental DC CB is set-up using another type of VCB as shown in Figure 3-17. The photo shows a double interrupter set-up. The ratings of all the VCBs used in the test campaign are shown in Table 1 in Chapter 2.

Similar tests duties were applied as for VCB Type A including the same current injection circuit. For VCB Type B the dispersion of the moment of contact separation of the VIs is significant and, thus the precise control of arcing duration is slightly challenging. The performance of VCB Type B is, however, completely different than the performance of VCB type A. In many test cases, the VCB Type B cleared the short-circuit current at the 1st CZC and, sometimes even at shorter arcing duration than VCB type A. In general, tests were performed 62 times of which on 47 occasions the VI(s) cleared on 1st CZC. Actually, of the total test shots, only 10 times the failure to clear was recorded. This slightly higher percentage failure than VCB type A.

This project has received funding from the European Union's Horizon 2020 research and innovation programme under grant agreement No 691714.

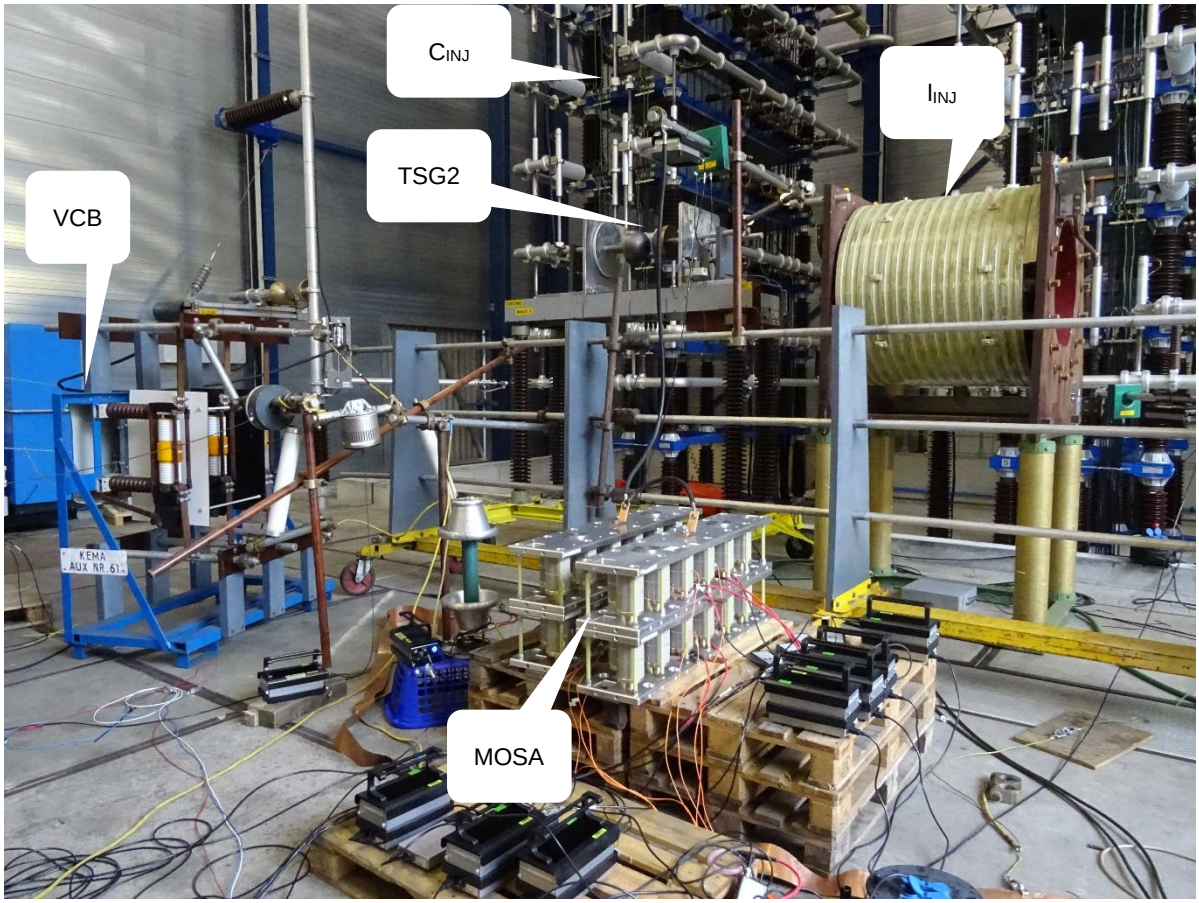

Figure 3-17: Laboratory set-up of double interrupter experimental DC CB using VCB Type B

3.1.6 TEST RESULTS ANALYSIS OF SINGLE INTERRUPTER EXPERIMENTAL DC CB – VCB TYPE B

Considering current interruption with test duty 1, no failed interruptions were observed. Tests were repeated 10 times with arcing duration ranging from 2.47 to 3.15 ms and in all the cases the VI cleared on the 1st CZC. Looking at the parameters near CZC, the di/dt is about 600 A/µs and the ITIV is 26 kV. In no occasion has a reignition or (late) restrike been observed during the series of test duty 1 interruptions. A typical test result of a test duty 1 current interruption is shown in Figure 3-18. After current interruption in the VI, the TIV rises from around -26 kV to peak value of 36.2 kV with average rate-of-rise (du/dt) of 0.064 kV/µs. The slow rate-of-rise of the TIV is due to the low system current which charges the injection capacitor after current interruption, see Figure 3-18b. The rate-of-rise is not an issue here although it is much lower than the rate-of-rise of voltage in AC (1.5-3.5 kV/µs, which is system dependent) rather the immediate voltage due to the remaining charge across

This project has received funding from the European Union's Horizon 2020 research and innovation programme under grant agreement No 691714.

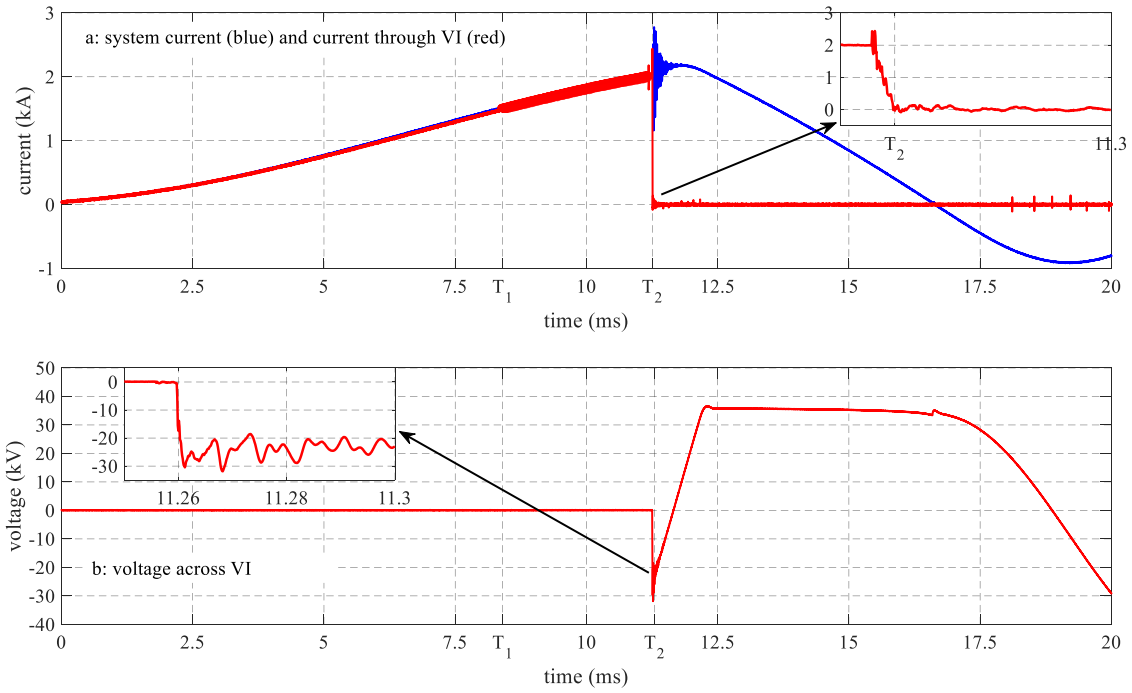

Figure 3-18: Typical test result using a VI of VCB Type B – Test duty 1 current interruption.

Test duty 2 (10 kA) current interruption was also performed 10 times using a single VI of VCB Type B. In 4 occasions the VI failed to clear even if up to 10 CZCs were created. Looking at the failure to interrupt test results, in all cases the failure to interrupt occurred due to too short arcing durations. This means that the VI could not achieve sufficient withstand capability in between the separated contacts during the period in which CZCs occurred. Specifically, the arcing duration until the 1st CZC was in the range from 0.33 ms to 1.73 ms although arcing duration until the last CZC is as long as 2.54 ms. Up to 10 reignitions per test are observed at this test duty although the reignition voltages at each CZCs are less than 3 kV except on one occasion where 20 kV ITIV is observed at the 1st CZC. The latter is observed for the longest arcing duration among the failed test cases, i.e. when the arcing duration until 1st CZC is 1.73 ms. The measurements showing the detail of the test result of this case is shown in Figure 3-19. An important observation from the test result shown in this figure is that the reignition voltage at later CZCs did not increase unlike for VCB Type A discussed in the previous section although some reignition voltages are observed at the subsequent CZCs.

Note that the too short arcing duration in these tests were not intentional rather it was due to the dispersion of the moment of contact separation of the VIs.

This project has received funding from the European Union's Horizon 2020 research and innovation programme under grant agreement No 691714.

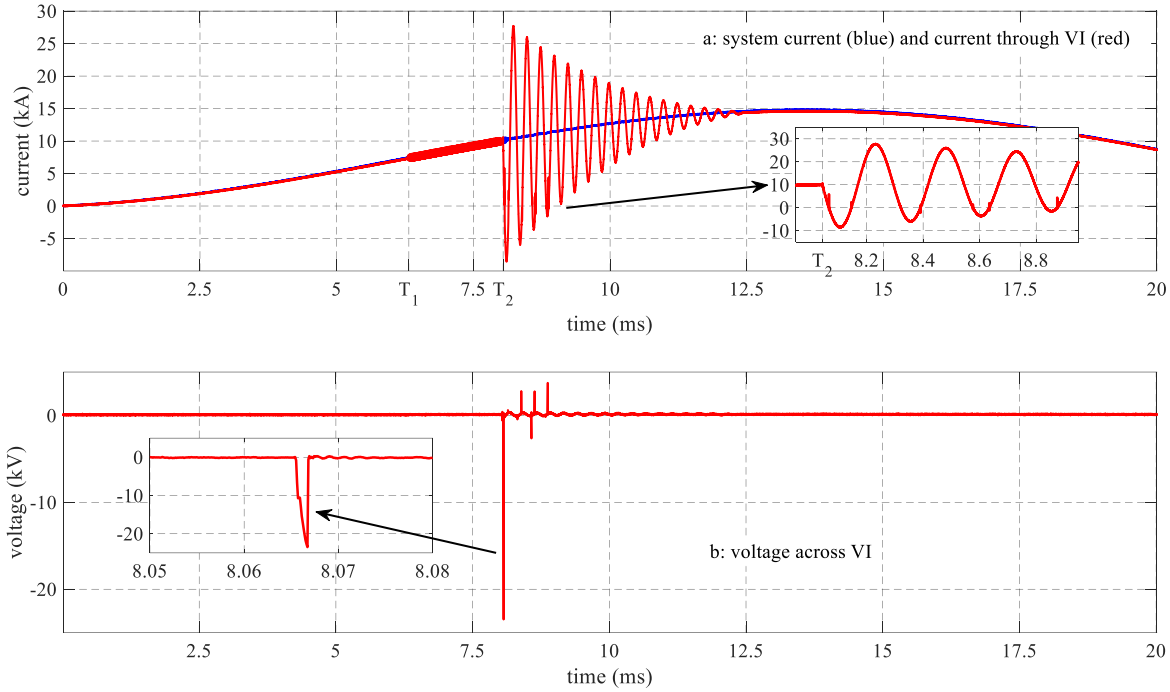

Figure 3-19: Test result showing failed interruption of test duty 2 by VCB Type B

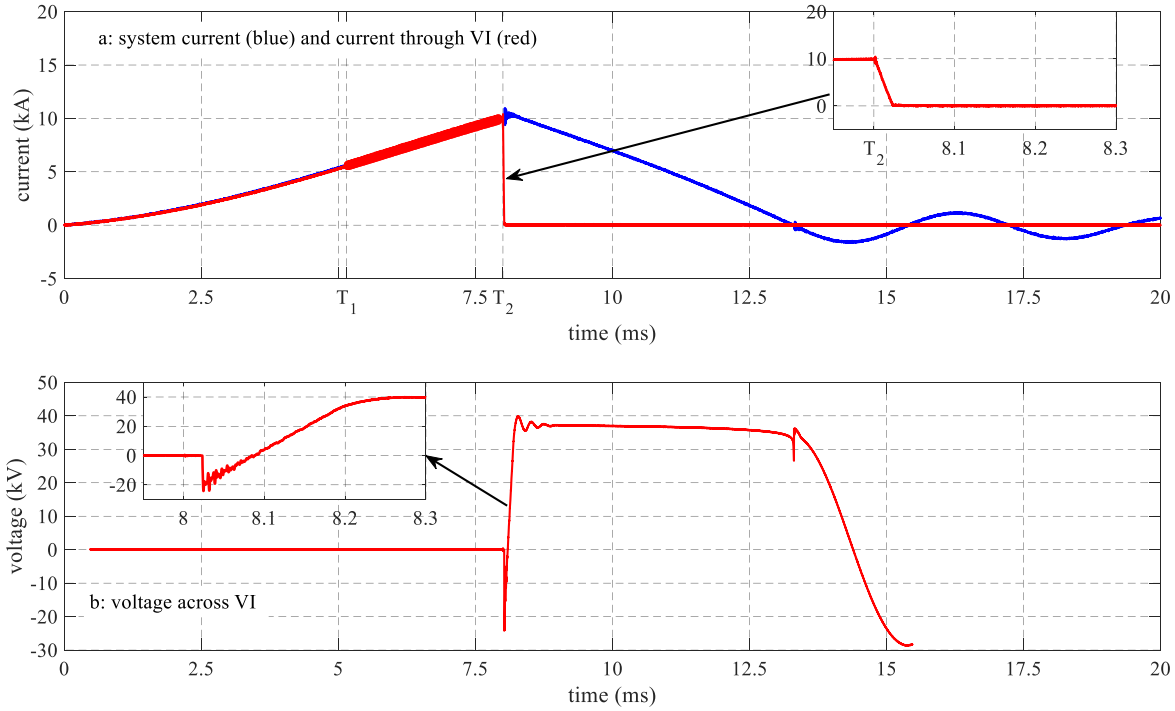

Figure 3-20: Typical test result showing test duty 2 interruption by VI of VCB Type B

Successful current interruptions are recorded in the remaining 6 test shots where in all cases interruptions occurred on the 1st CZC. In other words, all the tests in which the VI reignited at 1st CZC led to total failure to clear despite the chances at subsequent CZCs. In addition, there was no (late) restrike observed during the tests using

This project has received funding from the European Union's Horizon 2020 research and innovation programme under grant agreement No 691714.

a single VI of VCB Type B. A typical test result of such test cases is shown in Figure 3-20 where current interruption occurred after 2.85 ms arcing time on the 1st CZC.

The parameters near CZC for the test duty 2 are as follows; the di/dt is approximately 350 A/µs and the ITIV is 21.6 kV. After the current interruption, the TIV rises from -21.6 kV to 39.9 kV in about 0.25 ms with average du/dt of 0.25 kV/µs. The VI sustained the TIV of over 37.1 kV for about 5 ms without any restrike.

Next, the high-current test duty (test duty 3) was performed 12 times on a single VI of VCB Type B. In 50 % of the cases the VI failed to clear at this test duty even with arcing durations as long as 3.48 ms (until 1st CZC). At this test duty, a minimum of 4 CZCs are created using the injection circuit which remains the same for all test duties. Figure 3-21 shows test results of a failed current interruption of test duty 3 with arcing duration of 3.48 ms. Note that the arcing duration until the last CZC (4th) is 3.78 ms in this case. It can be seen from this figure that the VI attempted to clear at the first CZC and reignited at ITIV of about 20 kV. An attempt to clear is also observed at the 2nd CZC although the reignition occurred at a lower voltage (16 kV) than the 1st CZC. This is completely different for a VI of type A VCB where the reignition voltage is higher at CZCs following minor loop current (even CZCs).

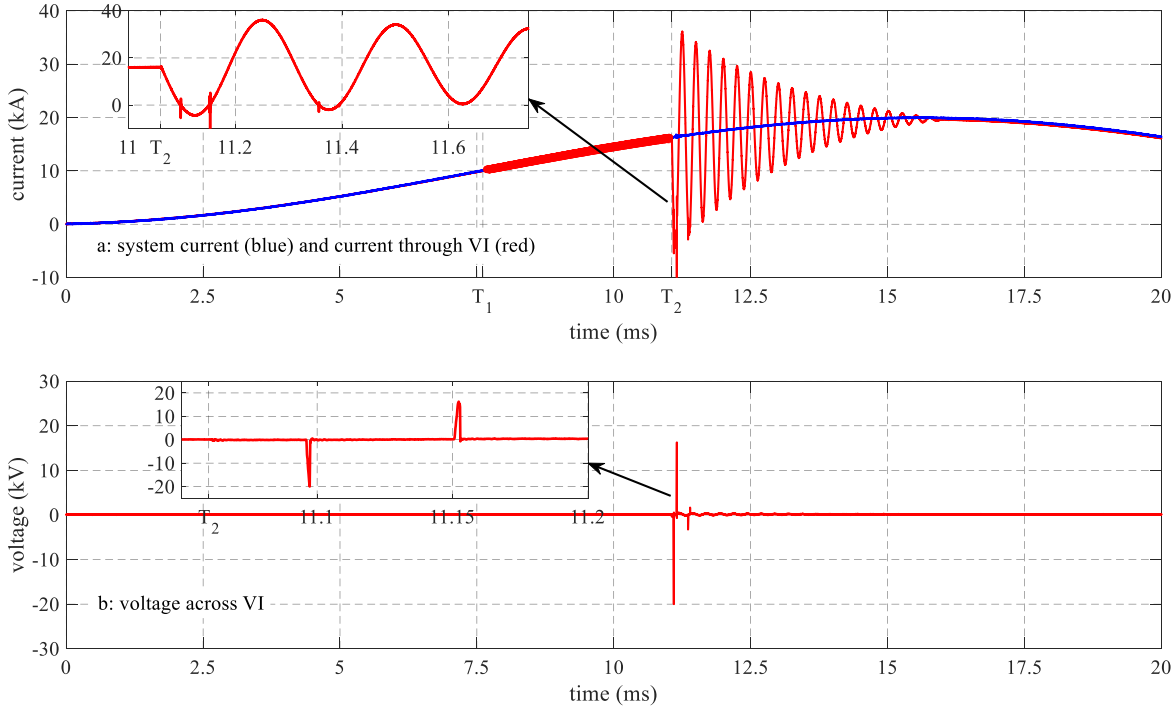

Figure 3-21: Test result showing failed interruption of test duty 3 by VCB Type B

A general observation from the failed test results is that as the arcing duration (until the 1st CZC) increases, the reignition voltages at CZCs also increase. This confirms the VI's attempts to clear improve with longer arcing duration. Successful current interruption was achieved when the arcing duration until 1st CZC is increased to 3.6 ms. All the tests with arcing durations longer than 3.6 ms resulted in successful interruption and, in all cases, upon the 1st CZC. The current interruption with arcing duration of 3.6 ms is shown in Figure 3-22. At the 1st CZC the di/dt is approximately 330 A/µs and the ITIV is 17 kV. The TIV rises to a peak value of 42.3 kV from -17 kV with average rate-of-rise of 0.4 kV/µs. Note the significant increase in the du/dt at this test duty compared to other test duties. Also, at high current test duty, the peak TIV is high due to V-I characteristics of the MOSA.

This project has received funding from the European Union's Horizon 2020 research and innovation programme under grant agreement No 691714.

The main conclusion from these tests is that longer arcing duration is needed as the magnitude of test duty currents increase. In other words, for a given rated current interruption there is minimum arcing duration that needs to be ensured before CZC creation for this VI.

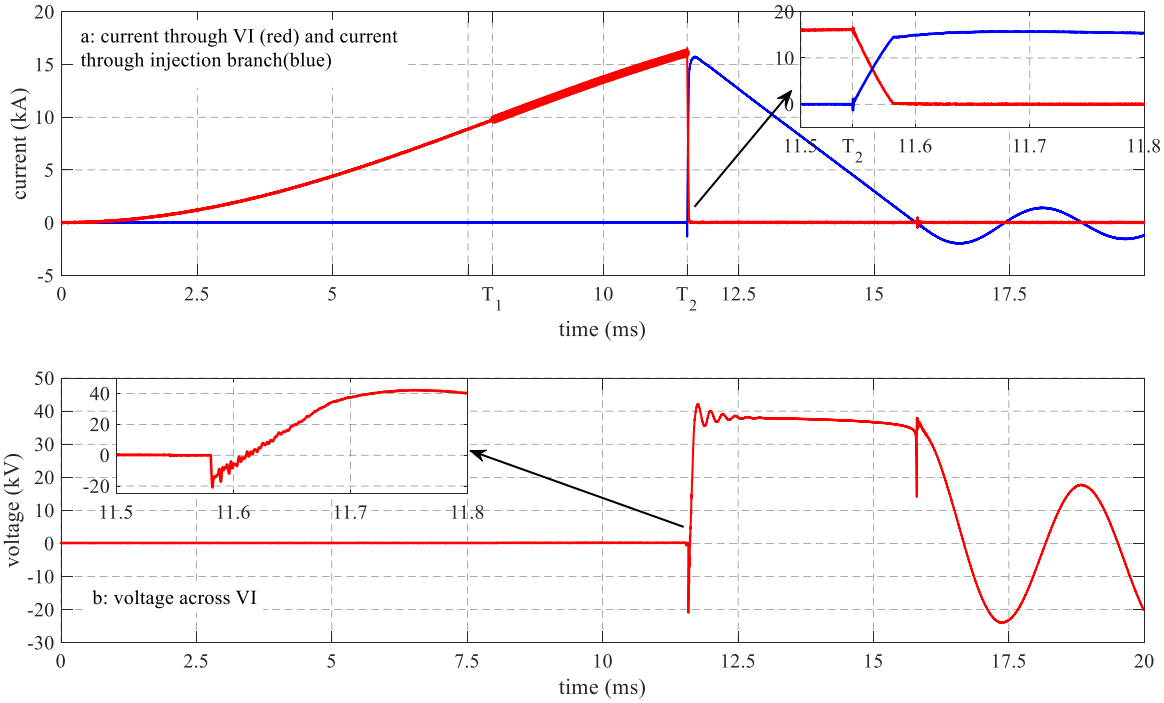

Figure 3-22: Typical test result showing successful test duty 3 interruption by VCB Type B (single interrupter)

3.1.7 TEST RESULTS ANALYSIS OF DOUBLE INTERRUPTER EXPERIMENTAL DCCB – VCB TYPE B

Two VIs of VCB type B are connected in series to investigate the performance at high voltage application. As for the single VI case, tests were repeated 10 or 11 times for each of the three test duties. No failures to interrupt were recorded when using double interrupter although a few reignitions and restrikes occurred at low current test duties. A critical observation during these series of tests is the voltage sharing issue between the two VIs even though 700 pF grading capacitors are placed across each VI.

Among the 11 tests at test duty 1, in 8 cases the VIs cleared at the 1st CZC with an arcing duration as short as 1.8 ms. The test duty 1 current magnitude was unintentionally set to 3 kA in this case. On one occasion current interruption occurred at the 2nd CZC. At this test, a total reignition voltage of 30.5 kV is measured across both VIs at the 1st CZC although only 3 kV appeared across one of the VIs (VI_1). VI_1 is the one across which the voltage measurement is placed.

In another test (same duty) a restrike occurred 0.45 ms after clearing at the 1st CZC. The test result of this case is shown Figure 3-23. The black trace shows voltage measurement across both VIs while the red trace shows the voltage across VI_1. The black trace shows the voltage measurement across both VIs while the red trace shows the voltage across only VI_1. From the zoomed sections of the graphs, it can be seen that both VIs cleared at the 1st CZC as the ITIV and, later the TIV is shared between the two VIs, see Figure 3-23b, although the voltage sharing is not perfectly equal. Then, both VIs re-struck simultaneously when the TIV reaches 60 kV (36 kV across VI_1 and 24 kV across VI_2). After the restrike, the superposition of the system current and the high-frequency

This project has received funding from the European Union's Horizon 2020 research and innovation programme under grant agreement No 691714.

discharge from the injection capacitor flows through the VIs. Several CZCs have been created until finally clearing at 22nd zero crossing. However, at the second current interruption only VI_1 cleared. This can be observed from the voltage traces since the two measurements overlap. After the TIV reaches its peak value the VI_2 starts to slightly share a portion of it during the remainder of the current suppression period.

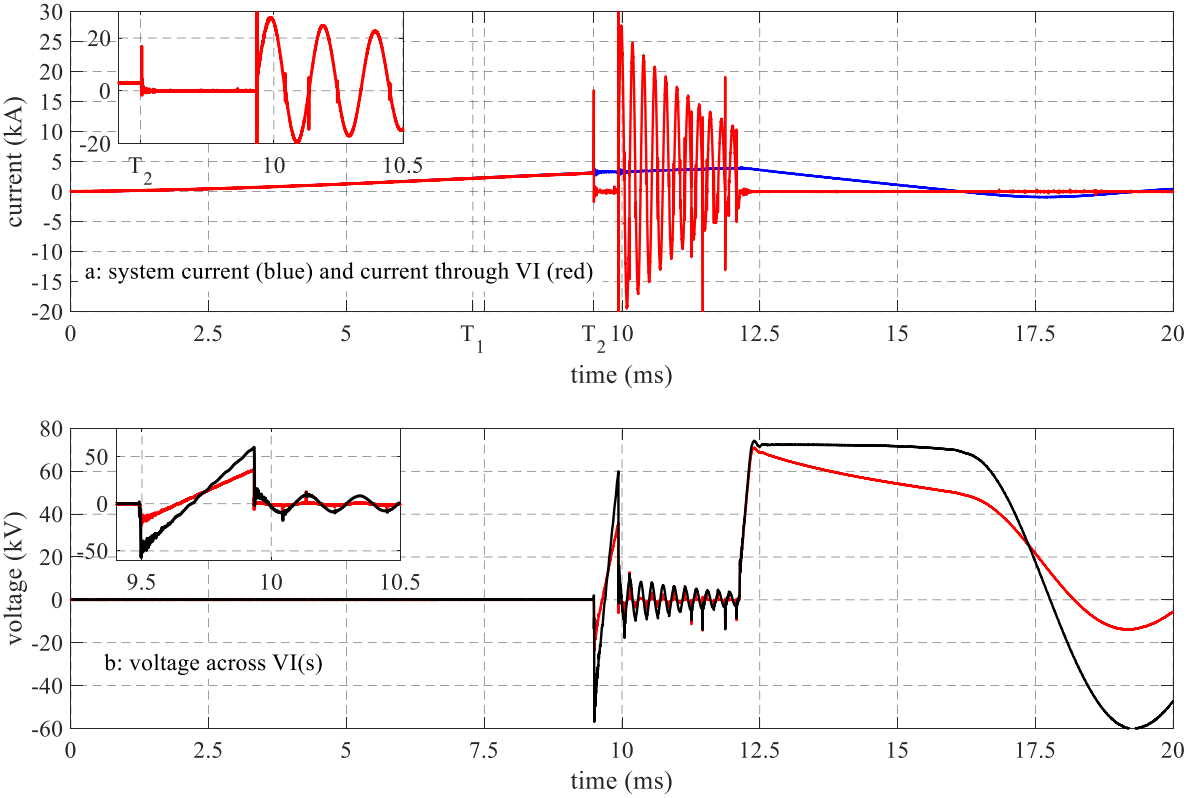

Figure 3-23: Test duty I current interruption by VCB type B. A restrike followed by several reignitions is observed before final interruption

During the test duty 2 current interruption series, only in one case a reignition occurred where the VIs interrupted at the 3rd CZC. In all the other cases interruption occurred at the 1st CZC. Similarly, there was no reignition or restrike observed during test duty 3 current interruption series. Current interruption occurred always at 1st CZC even if the arcing duration is as short duration as 2.07 ms although at arcing duration less than 3.5 ms a single VI could not clear current at test duty 3. In one test case the VI_2 reignited after 90 µs although this did not lead to overall reignition. This is shown in Figure 3-24. It can be seen from the zoomed section of Figure 3-24b that the VI_1 took over the entire TIV after the restrike in VI_2. A closer look at the voltage measurements shows that initially it was the VI_1 which cleared upon the CZC; however, as the TIV passes through zero (going from negative to positive) the TIV redistributes across the two VIs, see the black and red trace on zoomed section of Figure 3-24b. However, the VI_2 restrikes when approximately 30 kV is reached across its contacts. The later observation where initially one VI clears at the 1st CZC and the voltage sharing between the two VIs starts as the TIV goes from negative to positive was common throughout all the tests using this breaker.

PROMOTiON – Progress on Meshed HVDC Offshore Transmission Networks

This project has received funding from the European Union's Horizon 2020 research and innovation programme under grant agreement No 691714.

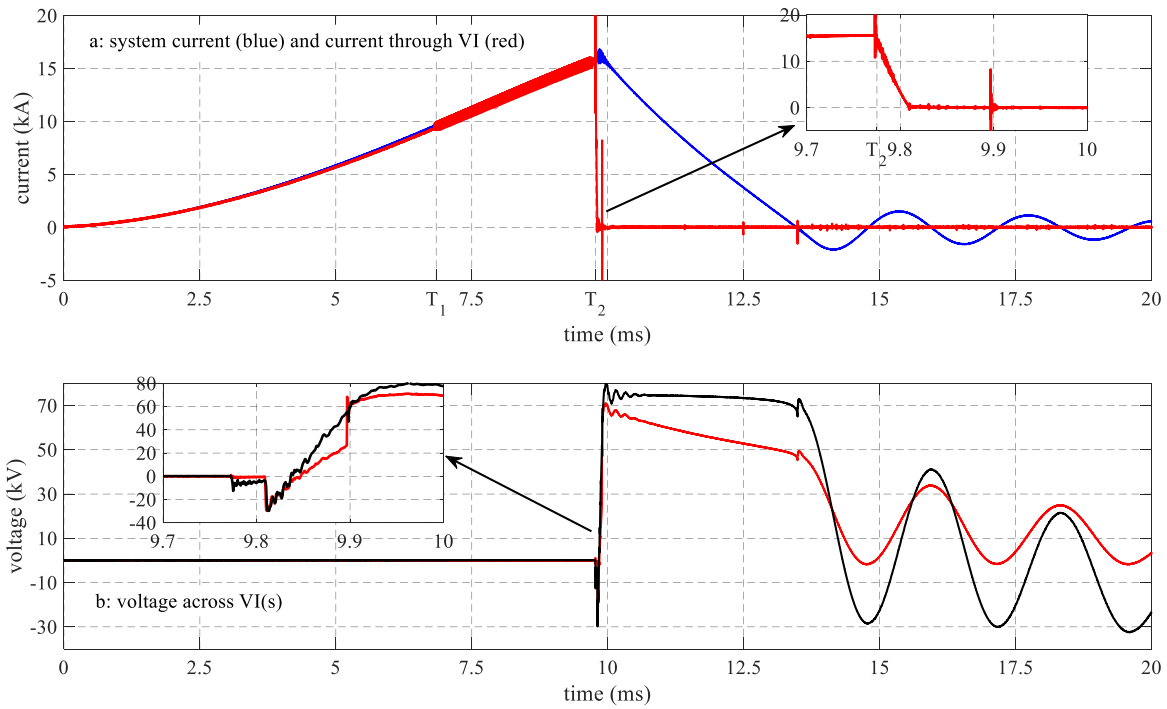

Figure 3-24: Test duty 3 current interruption by VCB type B

3.1.8 TEST RESULTS ANALYSIS OF SINGLE INTERRUPTER EXPERIMENTAL DC CB – VCB TYPE C

The third type of VCB (type C) is investigated in the experimental test campaign. A test setup with VCB type C is shown in Figure 3-25.

This project has received funding from the European Union's Horizon 2020 research and innovation programme under grant agreement No 691714.

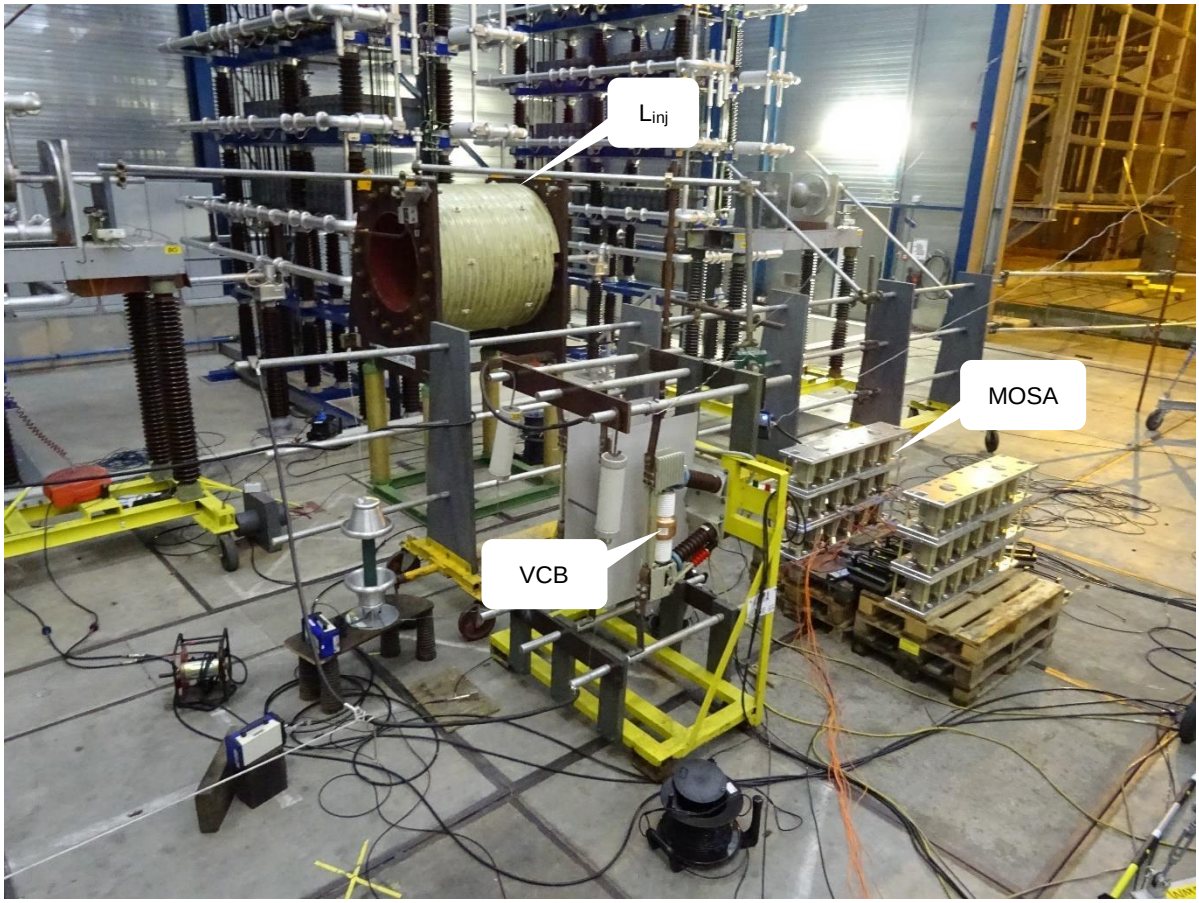

Figure 3-25: Lab set-up of experimental DC CB using VCB type C

3.1.9 TEST RESULTS ANALYSIS OF SINGLE INTERRUPTER EXPERIMENTAL DC CB – VCB TYPE C

For single interrupter test of this VCB, only test duty 2 has been performed at different arcing durations. Up to 10 test shots have been performed at this test duty with arcing duration ranging between 3.76 to 4.48 ms and, in all the cases the VI cleared on the 1st CZC. There was no restrike observed. However, when the arcing duration was reduced restrikes were observed on a couple of occasions which finally led to failed interruptions. With shorter arcing duration in the range between 0.3 to 1.6 ms, another series of 10 tests was performed. Similar to VCB type B, for this VCB the dispersion in the moment of contact separation is significant and the sub-millisecond arcing durations are the results of this dispersion.

Figure 3-26 shows a test result in which a restrike occurred in the VI of VCB type C. A restrike occurred not during the test case with the shortest arcing duration, rather during the test with the longest arcing duration (1.63 ms) in the series although a restrike was also observed in another test with arcing duration of 0.44 ms. The latter is also not the shortest arcing duration in the series. In both cases the VI failed to clear after the restrike even though 18 CZCs are created. In the test case shown in Figure 3-26, the VI has been opening for about 4.3 ms until the last CZC and it failed to clear. Similar phenomena, that the VI(s) fail to clear after reignition at the 1st CZC or after a restrike, were observed for the double interrupter tests using this VCB.

This project has received funding from the European Union's Horizon 2020 research and innovation programme under grant agreement No 691714.

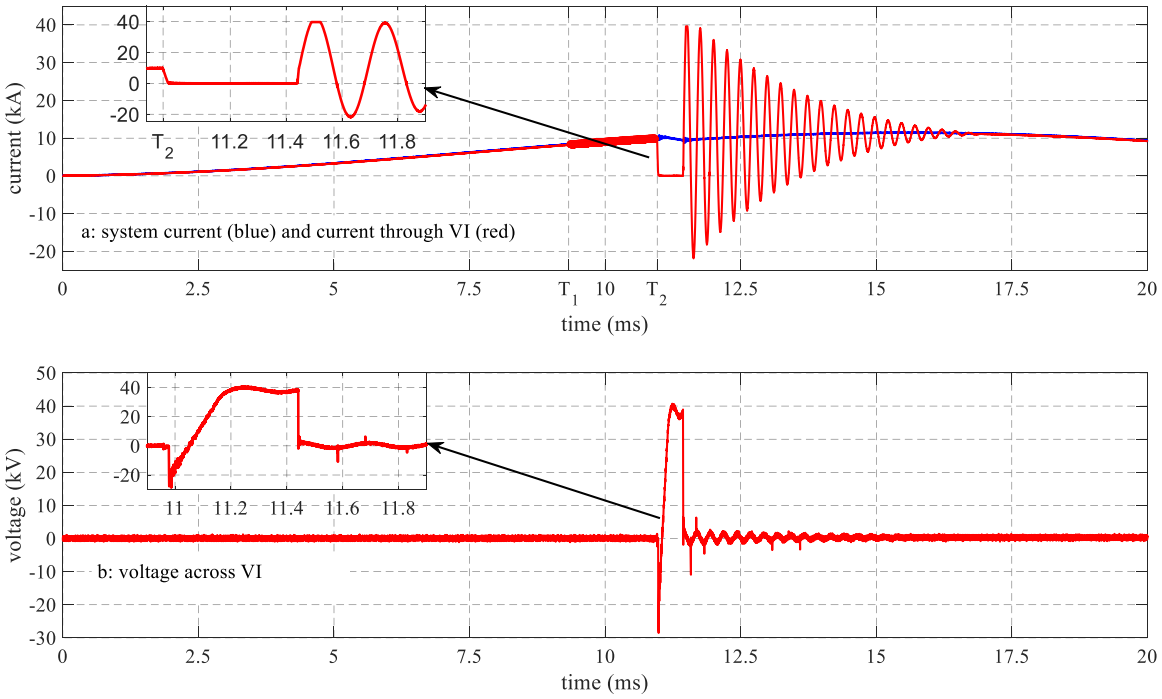

Figure 3-26: test duty 2 interruption by single VI of VCB type C. Restrike during current suppression period

3.1.10 TEST RESULTS ANALYSIS OF DOUBLE INTERRUPTER EXPERIMENTAL DC CB – VCB TYPE C

Similar to the other VCB types, the performance of a double interrupter DC CB composed of two VIs of VCB type C is investigated. However, in this case only test duties 2 and 3 are performed 5 and 6 times, respectively. The main difference with other double interrupter test set-ups (using VCBs type A and B) is that the voltage grading capacitors used in this set-up are 2500 pF, much larger than in the previous two cases where 700 pF grading capacitors are used. As a consequence of the increased grading capacitors, the voltage sharing has significantly improved resulting in almost equal voltage sharing.

Considering test duty 2, 5 test shots have been performed with arcing duration varying between 1.18 to 1.34 ms. In all cases the current is interrupted in the 1st CZC.

Test duty 3 is performed 6 times and only in one case a restrike and, subsequently, failure to interrupt occurred. A typical test result using double interrupter of VCB type C is shown in Figure 3-27. The arcing duration is set to 2 ms in this case. A very important point to note in this figure is the voltage sharing among the two VIs right from the moment of current interruption (see the zoomed section of Figure 3-27b). The VI_1 (see the red trace) takes about 51 % of the total voltage measured across both VIs (shown by the black trace). The remaining 4 test results with arcing duration of 2 ms also show quite similar voltage sharing.

PROMOTiON – Progress on Meshed HVDC Offshore Transmission Networks

This project has received funding from the European Union's Horizon 2020 research and innovation programme under grant agreement No 691714.

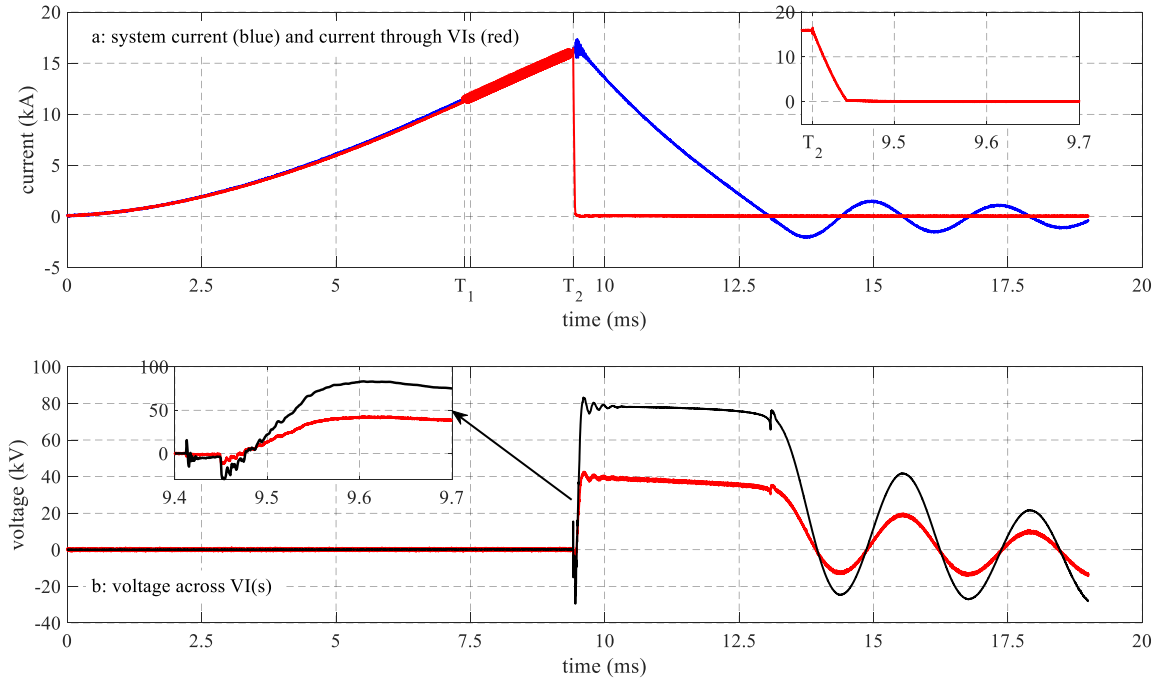

Figure 3-27: Test duty 3 current interruption by double interrupter VCB type C. Better voltage distribution using 2500 pF grading capacitor

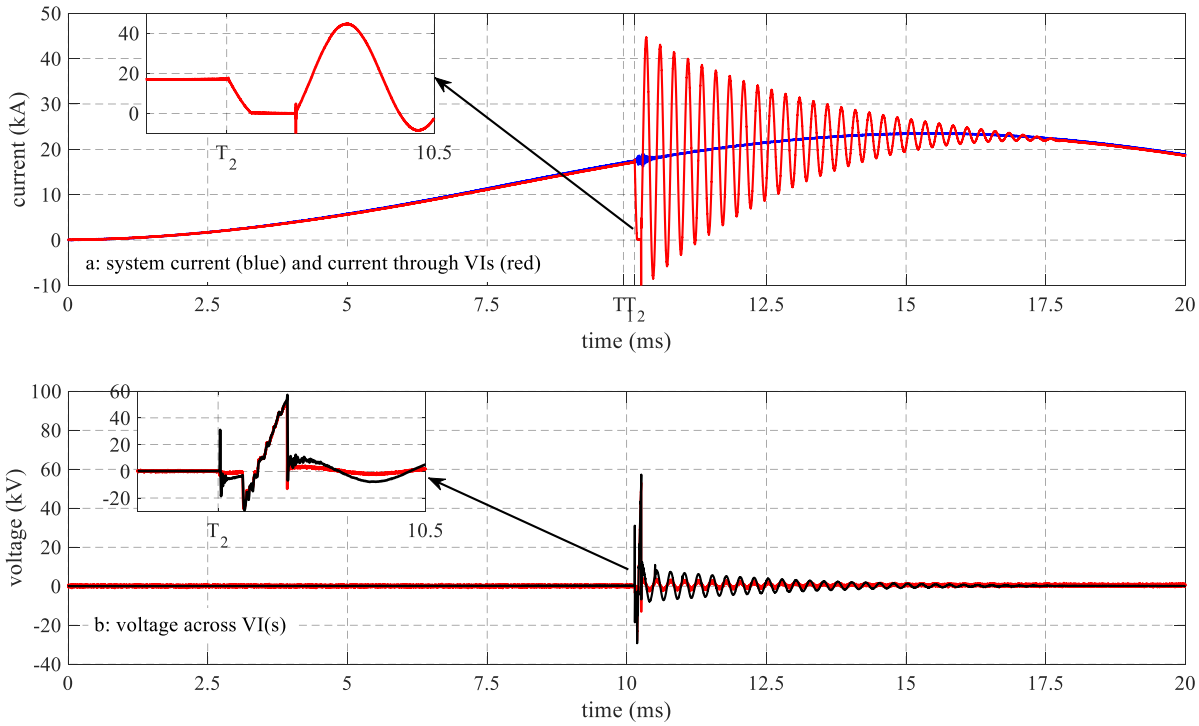

Figure 3-28: Test duty 3 failed current interruption by double interrupter VCB type C

Figure 3-28 shows a failed test duty 2 current interruption. In this case the arcing duration was extremely short, 0.2 ms. In this case only VI_1 cleared as can be observed from the voltage plots. The VI_1 sustained the ITIV of about 28 kV and it re-struck when the TIV rises to about 54 kV. In this case it could be possible that VI_2 could still

PROMOTiON – Progress on Meshed HVDC Offshore Transmission Networks

This project has received funding from the European Union's Horizon 2020 research and innovation programme under grant agreement No 691714.

be in a closed position while only VI_1 is clearing due to the very short arcing duration caused by the dispersion in the moment of contact separation. A very important observation similar to the single interrupter case of this VCB is that the VIs could not clear even if 8 CZCs are created after the restrike. This is typical observation for this VCB type.

The main conclusion from the above analyses is that the DC fault current interruption performance of VI based DC CBs depend on the design of the VI. In other words, there might be a possibility of optimizing the design of the VI for such an application.

3.2 MOSA STRESSES ANALYSIS

Another investigation during the experimental test campaign is on the performance of the MOSA for DC CB application. The focus in this case is on the energy absorption, current and energy sharing among the parallel columns as well as the temperature management of the MOSA columns. The details of the MOSA design procedure for DC CB application has been presented along with the major challenges, especially the column matching, in Deliverable 10.2, [7]. During the test campaign, several MOSA parameters were monitored and the following measurements were recorded:

- Total current through the MOSA
- Voltage across the MOSA
- Current through 8 columns of MOSA
- Temperature measurement of 8 columns of MOSA (the same columns as current measurement)
- Surface temperature monitoring through thermal imaging camera and infrared thermometer

Figure 3-29 depicts a typical test result showing current commutation to the MOSA branch. The negative voltage across the MOSA is the pre-charge voltage across the injection capacitor which is applied to the MOSA as well.

This project has received funding from the European Union's Horizon 2020 research and innovation programme under grant agreement No 691714.

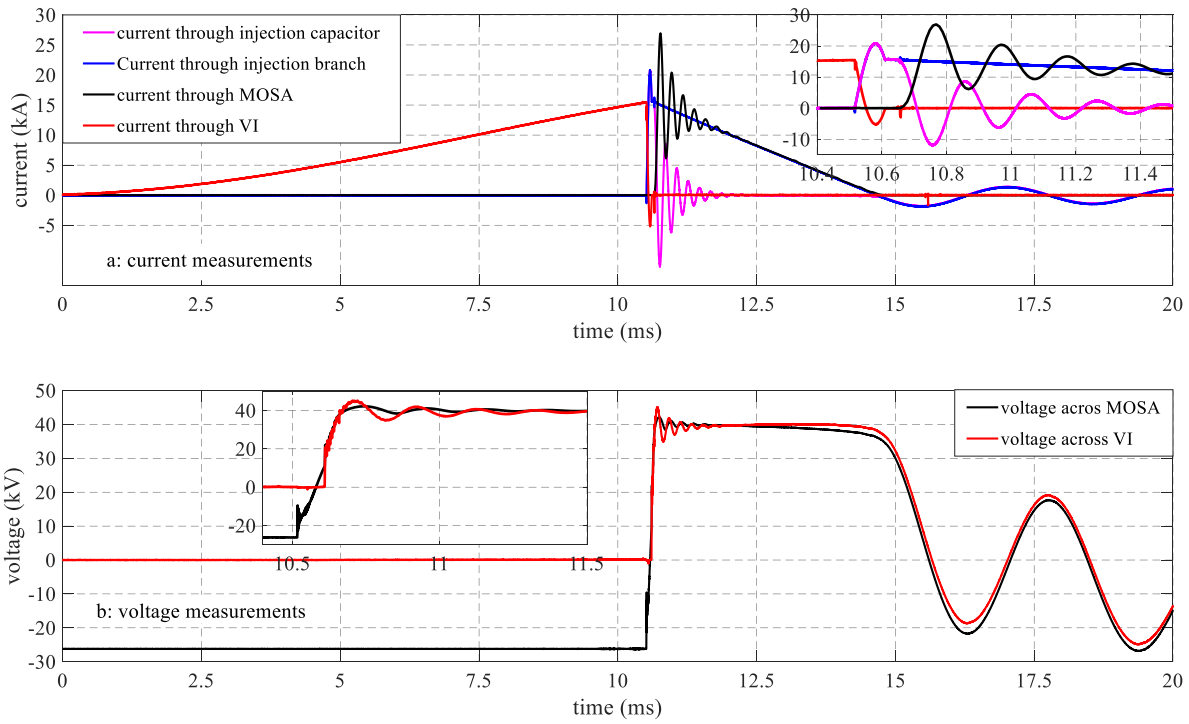

Figure 3-29: Internal current commutation of experimental DC CB – current though MOSA

First the current is cleared by the VI at the 2nd CZC. Then, the system current commutates to the injection branch, thus charging the capacitor. When the voltage across the capacitor reaches around 35 kV, the MOSA starts to conduct and hence, the system current commutates from the capacitor to the MOSA, see the magenta and black trace in the zoomed section of Figure 3-29b. However, the commutation does not stop by the time the MOSA current equals the system current. Instead the MOSA current continues to increase to a higher value than the system current. This is due to stray inductance in the loop between the injection capacitor and the MOSA. This results in circulating current between the capacitor and the MOSA branch which is observed on the decaying oscillation on the current measurements of the MOSA and the capacitor. This oscillation is not observed on the system current. Due to this circulating current, the charge across the capacitor, and hence the TIV, oscillates. Compact (low inductance) design of the set-up can reduce this oscillation. The difference in the voltage measurements across the VI and the MOSA is due to the voltage drop across the stray inductance.

The MOSA conducts current for about 4 ms in this case while maintaining the voltage above 36 kV. In doing so, the MOSA absorbs the energy of about 1.3 MJ from the system. In addition to the total current through the MOSA, the currents through 8 of its columns are also measured. Typical currents through MOSA columns are shown in Figure 3-30. It can be seen that the current through the MOSA columns are not equal. Especially, the deviation between the column currents increases as the temperature of the MOSA increases. The temperature difference is enhanced due to differences in cooling of MOSA columns caused by the arrangement of the columns. The columns located in the middle have less ventilation compared to the columns located at the edges. This was an observation form the test results.

This project has received funding from the European Union's Horizon 2020 research and innovation programme under grant agreement No 691714.

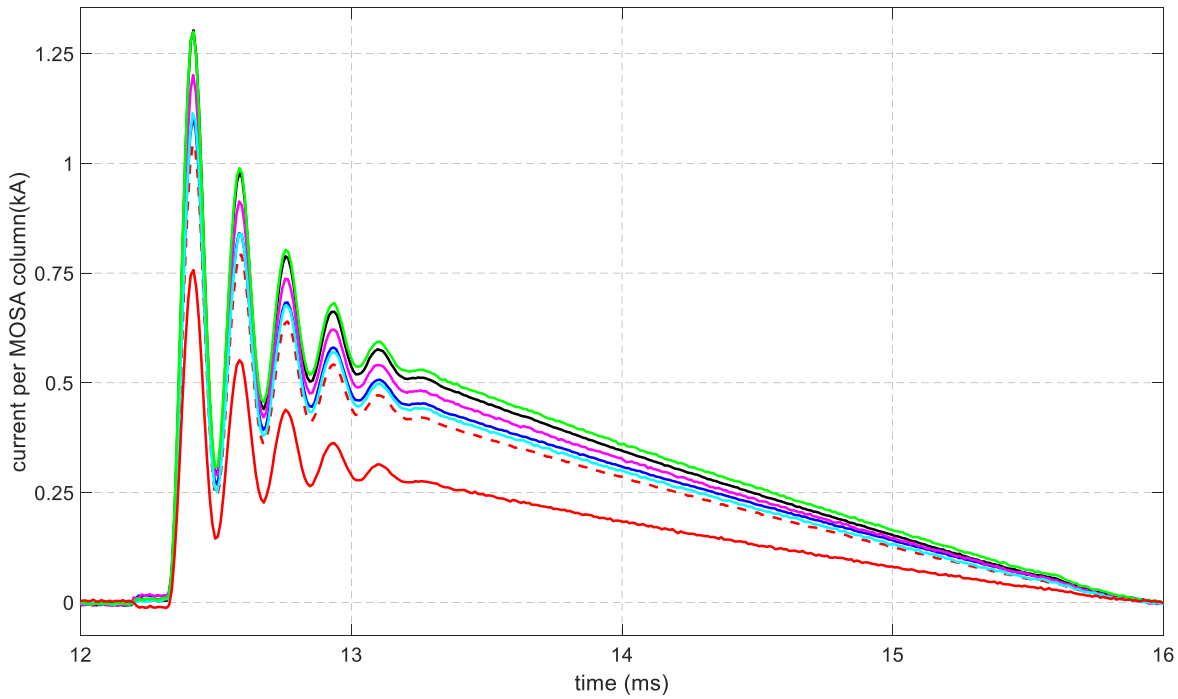

Figure 3-30: Typical current distribution among MOSA columns during energy absorption (current sharing issue)

In addition to the current and voltage measurements, the temperature of 8 columns of the MOSA is measured. Figure 3-31 shows the MOSA module with 8 fibre optic based temperature sensors mounted. The sensors are placed at the centre of each column as this is typically the hottest spot.

Figure 3-31: FO temperature sensor connections to MOSA columns

Figure 3-32a shows the MOSA temperature measurements by the FO sensors over 20 consecutive test shots. Tests were repeated until the temperature of the MOSA reaches around 170 ºC. The MOSA did not show any sign of failure. However, the temperature differences between the columns increase as the MOSA is heated by injection of energy while the increase in the temperature at a given energy injection slightly reduced. This can be seen from Figure 3-32b and c. Figure 3-32b shows temperature rise of 26 ºC in MOSA columns when 0.85 MJ

This project has received funding from the European Union's Horizon 2020 research and innovation programme under grant agreement No 691714.

energy is injected on the first test whereas Figure 3-32c shows temperature rise of about 21 ºC for approximately the same amount of energy except the initial temperature of MOSA in the latter case is around 130 ºC. This reduced temperature rise is due to the increase in heat capacity of MOSA with temperature.

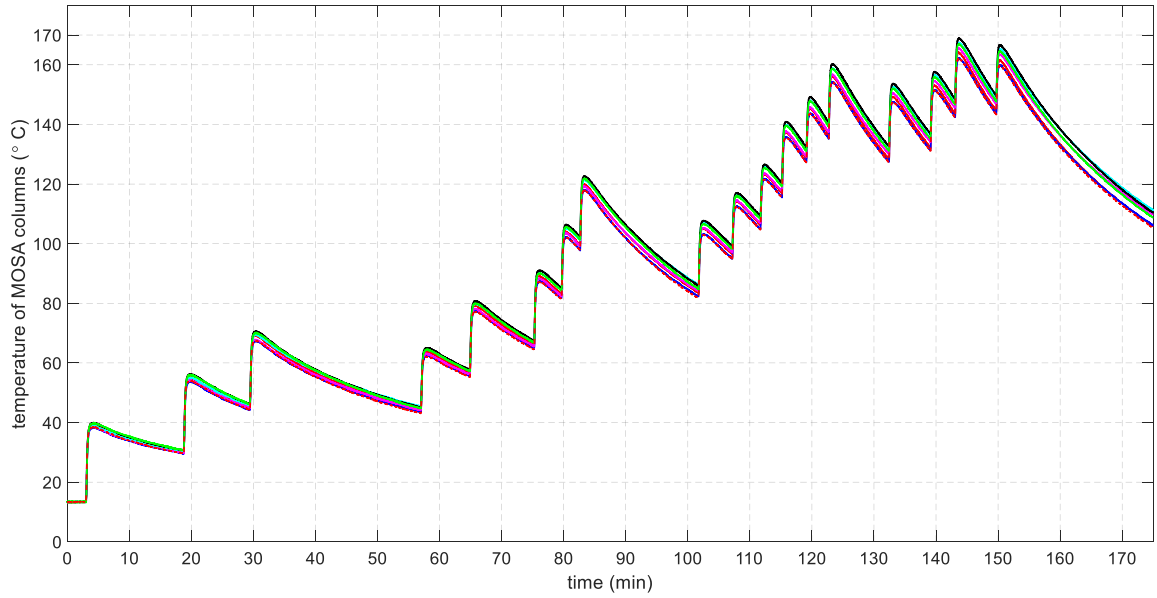

a)

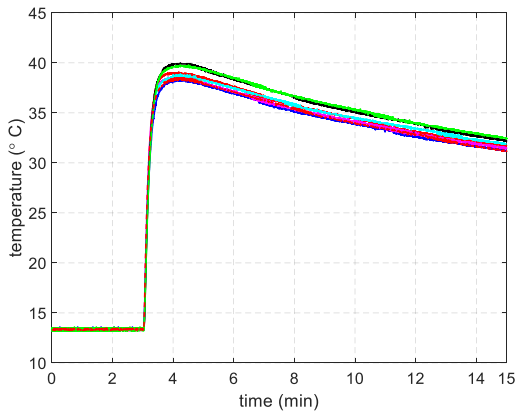

b)

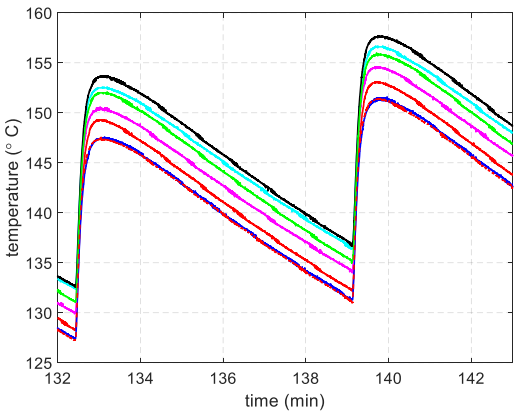

c)

Figure 3-32: MOSA temperature measurement during current interruption

Figure 3-33 and Figure 3-34 show the temperature reading captured by the thermal imaging camera at different times during the test campaign. It can be seen from the thermal images that the temperature distribution is uniform throughout the columns. In general, there was no occasion where extreme temperature differences or extreme current sharing issue is recorded.

This project has received funding from the European Union's Horizon 2020 research and innovation programme under grant agreement No 691714.

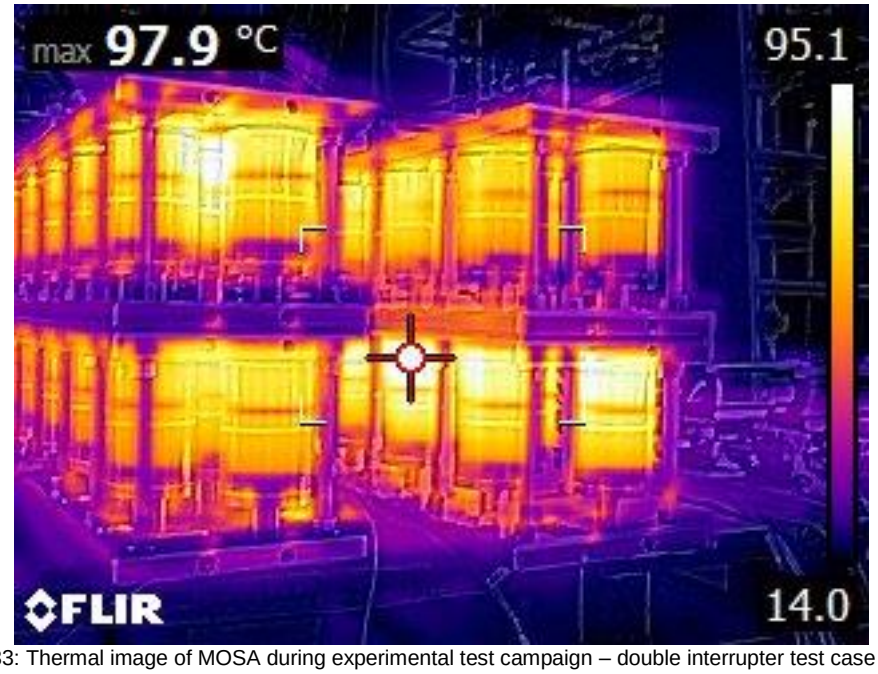

Figure 3-33: Thermal image of MOSA during experimental test campaign – double interrupter test case where two parallel sets are used

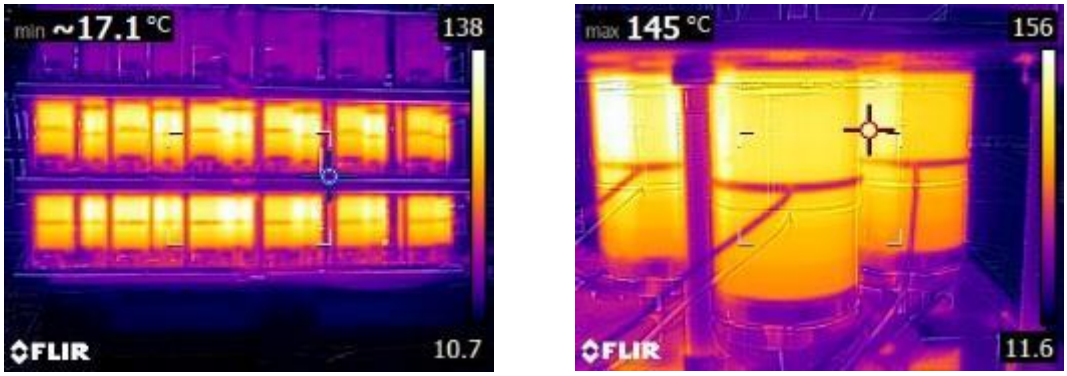

Figure 3-34: Thermal image of MOSA for double break DC CB

It must be noted that during the repeated energy injections discussed above, the maximum energy absorbed by MOSA at a time was about 1.3 MJ which is about half the amount it can handle. This was intended not to over heat the MOSA while repeating as many tests as possible within a short period of time. Later a few test shots were performed to inject 2.5 MJ energy per MOSA bank. This results in energy per volume of 200 j/cm^3 which assumed to be acceptable by MOSA.

A test result shown Figure 3-35 is one of the cases where high-energy absorption is performed. It can be seen that the MOSA is conducting current for about 10 ms which is usually long duration compared to its conventional application in AC systems. While MOSA is conducting or absorbing energy for about 10 ms, the TIV appears across the two VIs (since this was a double interrupter case) for the same duration. In this case the energy of about 5.3 MJ is absorbed by two series connected MOSA banks. This is shown in Figure 3-36.

This project has received funding from the European Union's Horizon 2020 research and innovation programme under grant agreement No 691714.

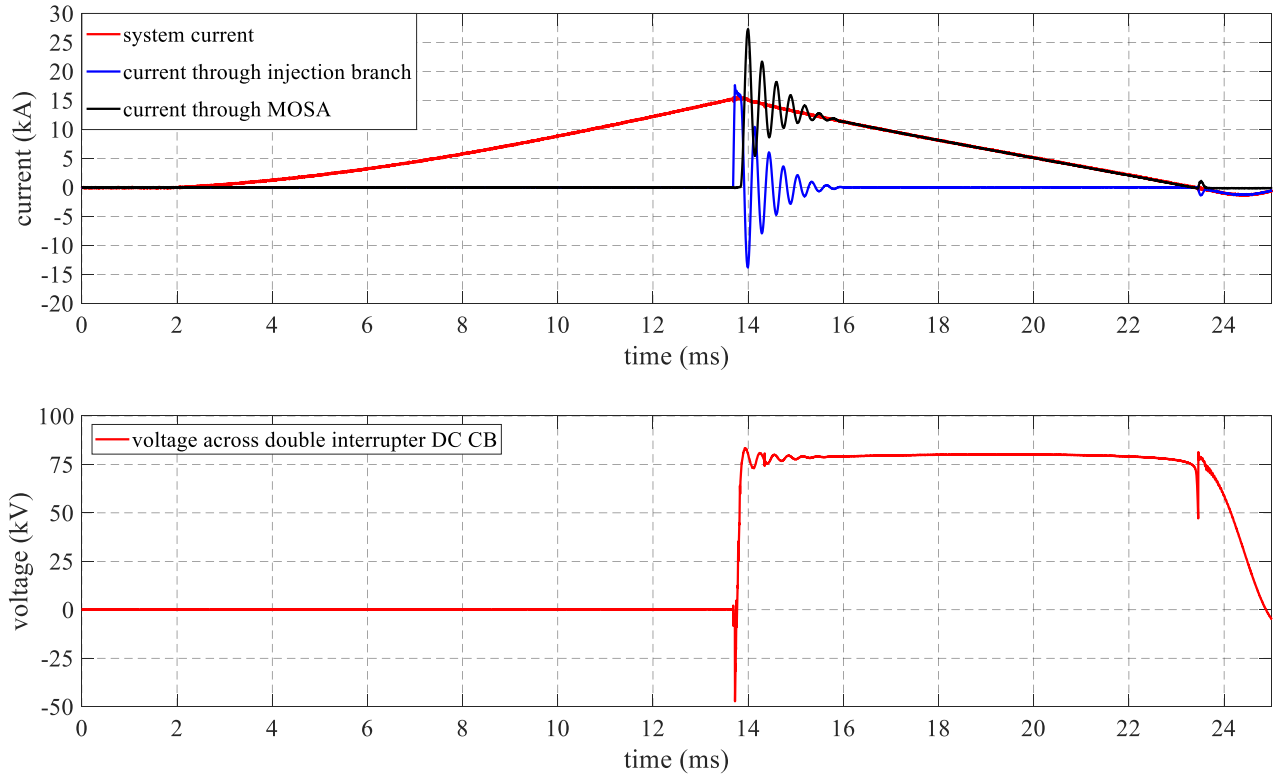

Figure 3-35: High-energy test result

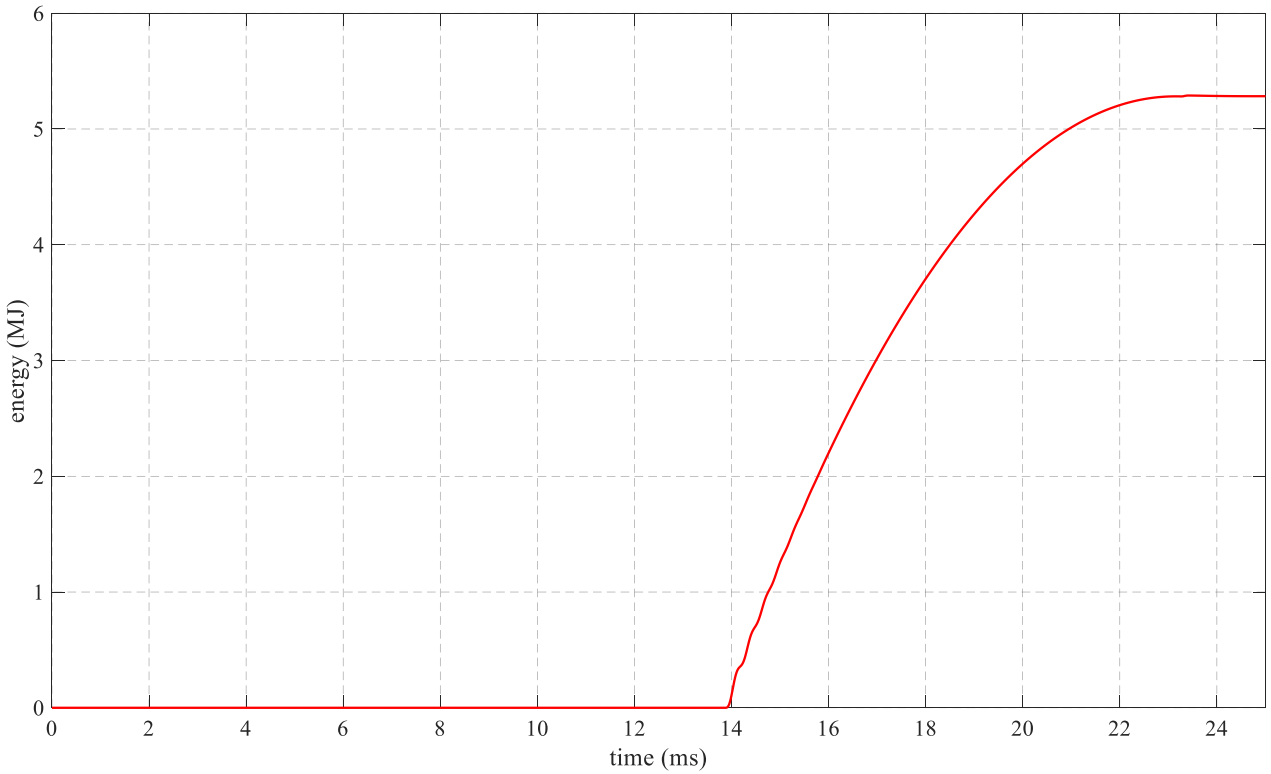

Figure 3-36: energy absorption by MOSA during high-energy test

This project has received funding from the European Union's Horizon 2020 research and innovation programme under grant agreement No 691714.

Figure 3-37 shows temperature rise across the MOSA during three successive high-energy absorption tests. In this case a temperature rise by 72 ºC is observed in the first test. In the next test temperature rise of 67 ºC is observed for nearly the same amount of energy. This shows that there is a change in the heat capacity of MO varistor discs with temperature. The higher the temperature, the higher the heat capacity. MOSA temperature raised to above 200 ºC. In the fourth test the MOSA actually failed to absorb energy where a few MO varistor disks exploded.

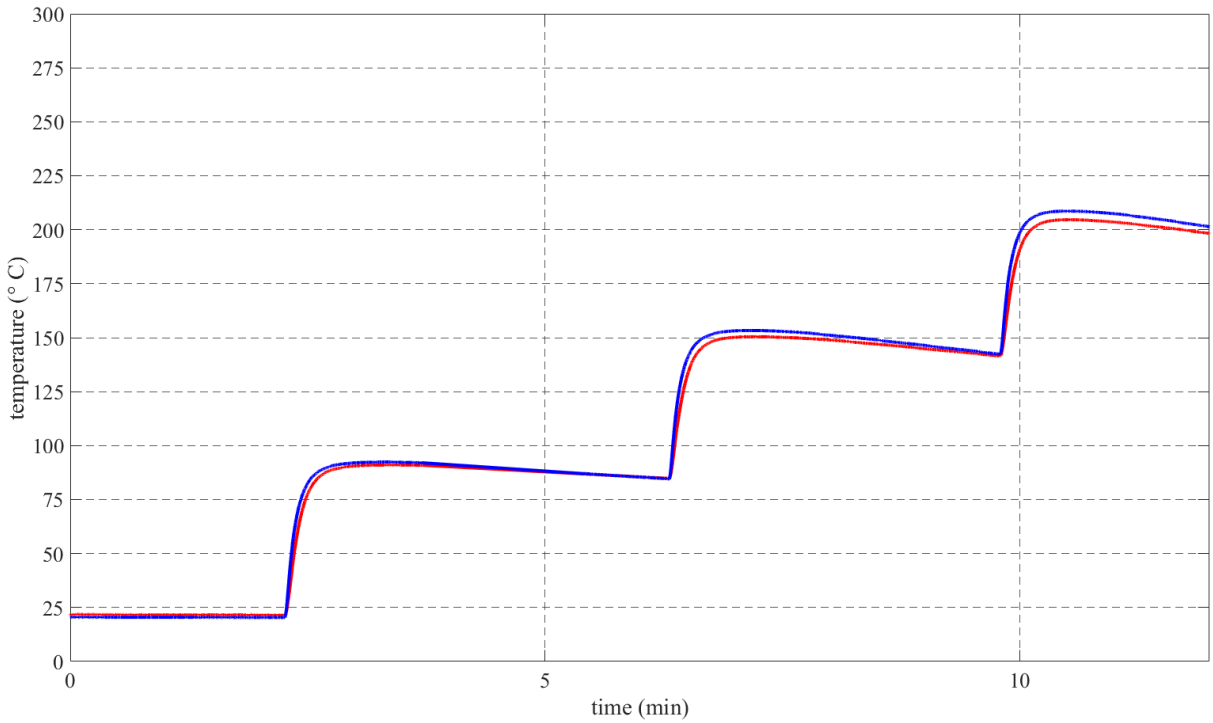

Figure 3-37: Temperature measurement during three successive high-energy tests.

The main conclusion here is that a good design of MOSA for DC CB application is essential. By over dimensioning for energy absorption it can be used for successive current interruption in short duration of time. A MOSA designer has to consider a temperature rise at a given energy absorption. Energy per volume of 200 J/cm^3 seems good for a few current interruptions. However, by computing the expected energy injection per current interruption it can be designed for several current interruption by over dimensioning or in other words by increasing the volume of MOSA available for energy absorption and hence, lowering the expected energy per volume. This is discussed in detail [7].

3.3 STATISTICAL ANALYSIS OF TEST RESULTS

Finally, the statistical performance of the three VCBs used in the test campaign is presented in Figure 3-38, where for each VCB type the total number of successful current interruptions and failed current interruptions (for both single and double interrupter set-ups) and the total number of success and failure per single as well as double interrupter set-ups are presented. For VCB type B, even if its performance at the 1st CZC is much better than that of VCB type A, the percentage of failure at single interrupter case is higher. This is due to the dispersion of the

This project has received funding from the European Union's Horizon 2020 research and innovation programme under grant agreement No 691714.

moment of contact separation which led to many too short arcing durations and, hence failures. However, the double interrupter experimental DC CB of VCB type B resulted in 100 % successful interruptions.

Considering the VCB type C, percentage failure is much lower than the other two VCBs. The failed interruption test cases have been evaluated for this VCB and in no occasion a failure was observed for arcing duration longer than 3 ms.

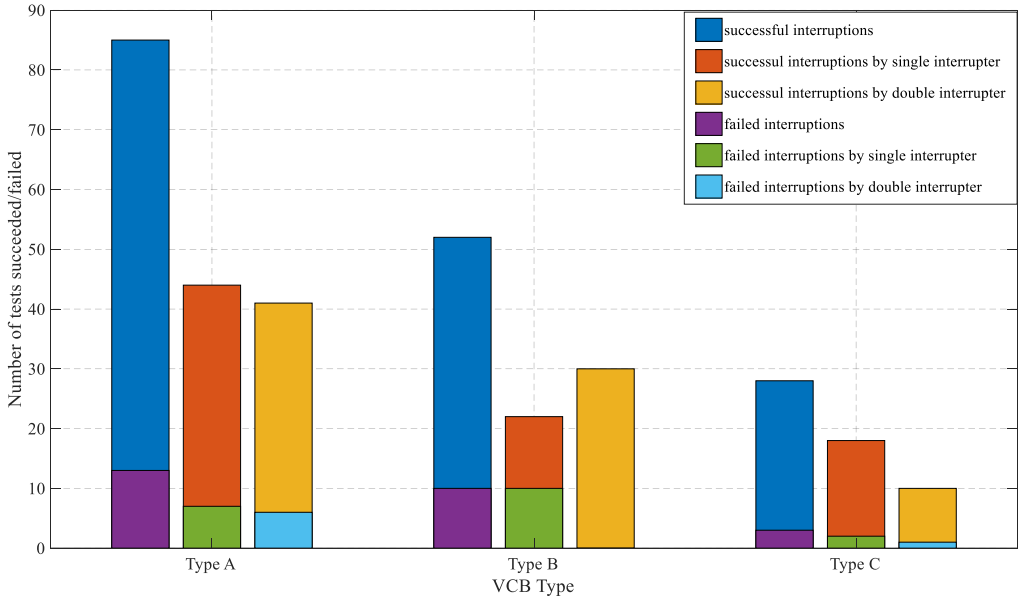

Figure 3-38: General test results statistical information

Looking at failed test cases of double interrupter made of VCB type A, it is mostly caused by unequal sharing of the TIV between the VIs. In all the cases where the TIV is shared fairly (within 40-60 % distribution), the tests resulted in successful interruption even at low arcing durations. This gives an indication that if proper voltage grading, among the series connected VIs, is ensured, enhanced performance can be achieved compared to a single interrupter case. The same observation can be made from a double interrupter test using VCB type B and C. For type B double interrupter case, there was no failed interruption recorded. For VCB type C, in one out of 11 tests a failure using double interrupter case is observed. The one test in which it failed interrupt is due to extremely short arcing duration caused by dispersion in the moment of contact separation.

This project has received funding from the European Union's Horizon 2020 research and innovation programme under grant agreement No 691714.

4 SUMMARY

This document provides detailed analysis of current interruption test results of an experimental DC CB with active current injection set-up in a test laboratory. First, the test arrangement of the experimental DC CB is discussed. Then, the test method and the test procedure are briefly presented.

Three test duties, namely, test duty 1, 2 and 3 with interruption current magnitudes of 2, 10 and 16 kA, respectively, are defined. Different configurations of a test circuit are designed to supply these test duty currents at different energy levels. The current interruption performances of three commercially available, different types of vacuum circuit breakers (VCBs) are investigated for the defined test duties. In fact, the investigation is only on the vacuum interrupters of these CBs. First, the parameters that have a strong impact on the current interruption performance of vacuum interrupters (VIs) are identified. These parameters include the duration of arcing until current zero crossing (CZC), the rate-of-change of current at CZCs, and the initial and the peak values of the transient interruption voltage (TIV). In addition, the possible events after CZCs such as reignition and restrike are discussed in detail together with their possible causes.

For the three different types of VCBs, two set-ups; the first using a single interrupter and the other is using double interrupters are arranged. All test duties are performed at least 10 times for each set-up and for each VCB type. As much as possible, the current injection circuit parameters remain the same for all the VCB types in order to make a fair comparison. Critical test results have been plotted and the detailed phenomena during the current interruption process are explained for each case.

Analysis of the test results shows that the three different types of VIs used in the investigation perform in a completely different manner when interrupting DC currents. This indicates a strong impact of the VI contact design, contact material and composition. For example, VCB type A, which is a 38 kV, 31.5 kA AC VCB, rarely interrupts current on the first CZC regardless of the length of arcing duration. This VCB mainly interrupts the current on the even numbered CZCs which occur after minor loop (half cycle) current flow. On the other hand, the VCB type B, which is a 36 kV, 40 kA AC VCB, mainly clears on the 1st CZC. Reignitions occurred only on a few occasions and were subsequently cleared on later CZCs. Moreover, the third type of VCB, which is 36 kV, 31.5 kA AC VCB, only clears on the 1st CZC. It never cleared when reignition occurred on the 1st CZC or when a restrike occurred afterwards. To illustrate these and other conclusions, a statistical analysis of the test results is presented. Form the statistical analysis it is observed that the performance of double interrupter set-up is better than the performance of a single interrupter case. The main cause of failure in the double interrupter set-up is the unfair distribution of TIV across the series connected VIs. This is specially observed when using VI type A. The main conclusion from this investigation is the fact that the vacuum interrupters can be optimized for DC current interruption.

The stresses on the metal oxide surge arrester (MOSA) during current interruption are also analysed in detail. A robust design of MOSA for DC CB application is essential. Custom-made MOSA banks, allowing the measurement of temperature and current through the individual surge arrestor columns, were used for the realisation of the experimental DC CB. Current sharing among the MOSA columns and the temperature of the MOSA after successive current interruptions are discussed. It is found out that the MOSA could sustain energy injection even after heated to more than 200 ºC. Due to a very robust design of the MOSA there was not significant

This project has received funding from the European Union's Horizon 2020 research and innovation programme under grant agreement No 691714.

current sharing deviation observed during the tests. Another important conclusion is that by providing sufficient margin for energy absorption several current interruptions and hence energy absorption can be achieved in quick succession.

This project has received funding from the European Union's Horizon 2020 research and innovation programme under grant agreement No 691714.

5 BIBLIOGRAPHY

[1] PROMOTioN Deliverable 10.1, “Test Report Describing Correct Functioning of Test Circuits,” PROMOTioN Project, 2018.

[2] PROMOTioN Deliverable 5.6, “Software and analysis report on candidate test-circuits and their effectiveness,” PROMOTioN Project, 2017.

[3] PROMOTioN Deliverable 5.7, “Realization of test environment for HVDC circuit-breakers,” PROMOTioN Project, 2017.

[4] P. G. Slade, The Vacuum Interrupter: Theory, Design and Application, CRC Press Taylor & Francis Group, 2008.

[5] K. Tahata, S. Ka, S. Tokoyoda, K. Kamei, K. Kikuchi, D. Yoshida, Y. Kono, R. Yamamoto and H. Ito, “HVDC circuit breakers for HVDC grid applications,” in *CIGRÉ AORC Technical meeting*, Tokyo, Japan, 2014.

[6] T. Heinz, V. Hinrichsen, L.-R. Jänicke, E. D. Taylor and J. Teichmann, “Direct current interruption with commercially available vacuum interrupters,” in *XXVI Int. Symp. on Discharges and Electrical Insulation in Vacuum*, Mumbai, 2014.

[7] PROMOTioN Deliverable 10.2, “Report Describing the interaction of Test Objects with the Test Environment,” PROMOTioN Project, 2018.

[8] L. Ängquist, S. Norrga and T. Modeer, “A new dc breaker with reduced need for semiconductors,” in *2016 18th European Conference on Power Electronics and Applications (EPE'16 ECCE Europe)*, Karlsruhe, 2016.

[9] L. LILJESTRAND, M. BACKMAN, L. JONSSON, M. RIVA and E. DULLNI, “DC VACUUM CIRCUIT BREAKER,” in *24th International Conference on Electricity Distribution*, Glasgow, 2017.

[10] S. Tokoyoda, K. Tahata, K. Kamei, K. Kikuchi, D. Yoshida, S. Oukaili, R. Yamamoto and H. Ito, “DC circuit breakers for HVDC grid applications HVDC and Power Electronics technology and developments,” in *CIGRE SC A3 & B3 joint colloquium, No.122*, 2015.

[11] W. Zhou, X. Wei, S. Zhang, G. Tang, Z. He, J. Zheng, Y. Dan and C. Gao, “Development and test of a 200kV full-bridge based hybrid HVDC breaker,” in *," in 17th European Conference on Power Electronics and Applications (EPE'15 ECCE-Europe)*, Geneva, Switzerland, 2015.

This project has received funding from the European Union’s Horizon 2020 research and innovation programme under grant agreement No 691714.